Elsevier Editorial System(tm) for Tectonophysics
Manuscript Draft

Manuscript Number: TECTO9706R1

Title: Basin formation by thermal subsidence of accretionary orogens

Article Type: Research Paper

Keywords: basin; accretionary crust; thermal subsidence; juvenile

Corresponding Author: Dr. Mark Allen,

Corresponding Author's Institution: Durham University

First Author: Peter Holt

Order of Authors: Peter Holt; Mark Allen; Jeroen Van Hunen

Abstract: Subsidence patterns of 18 stratigraphic sections from five sedimentary basins around the world are analysed by forward and inverse modelling, in order to explain the mechanisms by which basins form on the juvenile crust generated by accretionary orogens. Study areas are the Paraná Basin (Brazil), Karoo Basin and Cape Fold Belt (South Africa), the Arabian Platform, Scythian and Turan platforms (Central Asia) and eastern Australia. The form of the tectonic subsidence curves derived from backstripping analysis is consistent with results from a forward model, which produces thermal subsidence of crust with normal thickness (~35 km) but low initial mantle lithosphere thickness. This high thickness ratio of crust:mantle lithosphere is the plausible initial configuration of lithosphere produced by accretionary tectonics. Our results do not require late stage orogenic extension or lithosphere delamination as a precursor to the thermal subsidence phase.

*Abstract
Click here to download Abstract: Holt et al 2014 abstract.docx

Abstract

Subsidence patterns of 18 stratigraphic sections from five sedimentary basins around the world are analysed by forward and inverse modelling, in order to explain the mechanisms by which basins form on the juvenile crust generated by accretionary orogens. Study areas are the Paraná Basin (Brazil), Karoo Basin and Cape Fold Belt (South Africa), the Arabian Platform, Scythian and Turan platforms (Central Asia) and eastern Australia. The form of the tectonic subsidence curves derived from backstripping analysis is consistent with results from a forward model, which produces thermal subsidence of crust with normal thickness (~35 km) but low initial mantle lithosphere thickness. This high thickness ratio of crust:mantle lithosphere is the plausible initial configuration of lithosphere produced by accretionary tectonics. Our results do not require late stage orogenic extension or lithosphere delamination as a precursor to the thermal subsidence phase.

*Revision Notes
Click here to download Revision Notes: Response to referees of Holt et al JvH.docx

Response to referees of Holt et al.

We thank the three referees for their extremely helpful comments on the submitted paper, and appreciate the time that must have been needed. We have paid close attention to their suggestions, and feel that the revised paper greatly benefits from the constructive criticism. We take each referee's comments in turn, below, and offer a point-by-point account of how we have addressed them in the revised version. Our responses are preceded by the # symbol and are in italics.

1. Five basins were chosen for the analysis. Why were these basins chosen? The main goal of this paper is to show that a lithosphere cooling model is a fundamental process in accretionary orogens. Therefore, the choice of the case studies needs to be carefully justified to show that these are 'typical' basins (i.e., there are no special conditions that could lead to a subsidence pattern similar to that of the cooling model). This is done in places in the manuscript, but it should be more explicit. At the moment, it isn't clear if the five basins are representative of accretionary orogens or if they were chosen because they fit the cooling model.

#Text added to the introduction of the paper to reinforce and clarify the choice of basins: " Basins were chosen because they are large, representative features for which data are available; there was no filtering of locations to try and find the best fits to the proposed model". We also selected regions which have not been subjected to such a strong later tectonic overprint that the present day crust and lithosphere thickness values are completely unrepresentative of the conditions at the end of basin development. This is subjective: all regions have arguably undergone some kind of modification since the end of basin development, but we have consciously avoided using sections from basins now highly deformed and in the middle of major mountain belts, for example. See also the response to point #4, below.

2. The cooling model is only vaguely described and no quantitative details are provided. Perhaps there should be a separate section with a conceptual description of the cooling model - why is it expected that accretionary crust has a thin initial lithosphere, what maintains the thin lithosphere, and what happens to cause the lithosphere to start to cool? It is stated that this model is different from a mantle delamination model (top of pg 4), but the 'alternate' mechanism for creating thin lithosphere is not clearly described.

#Text has been added to explain the cooling model in section 2. There is also a longer description of why accretionary crust starts with thin mantle lithosphere in the Introduction. Both of these items were first described in Holt et al (2010): the only reason they were not originally given more length in this paper is that we thought readers would prefer a terse version of the material!

In addition, the actual numerical values used in the cooling model need to be given. Readers are referred to the Holt et al. (2010) paper, but it isn't clear how this method was applied to the current study. For example: Do all regions start with a 20 km thick mantle lithosphere or does this vary (as implied on pg 15, line ~18: "an unusually thin initial lithosphere…is required")? How was crustal thickness varied and do all regions have an equal thickness of upper and lower crust? Are the same thermal parameters used for all the regions? Please explain and justify the choice of parameters.

#Numerical values are now given in the text. Thermal parameters are kept constant, but the crust and initial lithosphere thickness are varied to produce the best fit to the observed subsidence pattern. This was noted in the original text, but has been made clearer (in the Method section).

3. There needs to be an explanation of the relationship between the 'zero time' of the numerical model (onset of cooling) and the geological time of the tectonic subsidence data. Presumably the initial elevation of most regions starts above sea level and after some time it subsides below sea-level (so there is some delay between the start of cooling and the onset of sedimentation). How was the time delay determined for each subsidence curve? The initial elevation should depend on what was chosen as the reference column for the isostatic balancing - please state what reference column was used.

#The reference column is now explained in section 2, and, as noted, the initial crustal and lithosphere thickness values were allowed to vary until the best fit with the subsidence data was obtained. The referee is right that regions typically start above sea level and there is a finite time before they subside below sea level. We have not stressed this part of the curves or represented them in the figures because we have no way of comparing them with real data – unlike the subsidence below sea level, which is represented by the accumulation within the basin. The delay time between initial subsidence and subsidence below sea level is on the order of a few 10s of million years in each case, or less. The magnitude of the initial height above sea level is typically 1000 m or less. This is all now explained in the revised text (Section 4.1).

4. Related to the above, the 'final' lithosphere structure is given for each region in Figure 3-7 captions (and discussed in the text) - does this correspond to the thickness at present-day (i.e., 0 Ma) or at the latest geological time of each plot or the last time of subsidence data (e.g., either -350 Ma or -300 Ma in the top plot of Fig 4). If it is one of the latter two, how can the lithosphere thickness be compared to the seismically-derived (0 Ma) thickness (e.g., pg 15, line 33)? It seems like some curves have not reached steady-state (e.g., top plot in Fig 4), so will continue to cool and thicken to present-day. If the 'final' structure is at present-day, the comparison between the cooling model and the seismic crust/lithosphere structure is questionable, as all of these regions have been affected by tectonic events since the end of the cooling models. For example, the South Africa region experienced extensive Jurassic magmatism (the Karoo large igneous province and kimberlites), which should have modified the lithosphere.

#We've modified the text to make it clearer that we have to use present values of crust and lithosphere thickness, and that these are not necessarily the same as the values at the end of the modelling (towards the end of the Method section). However, as noted above, we tried to select regions that have not been involved in so much tectonism since the end of basin formation that the original subsidence patterns cannot be deciphered or modelled. This is partly subjective: we have included a couple of subsidence curves that do not seem to fit our model toward the end of their lifespans (e.g. in eastern Australia), but in each case we have discussed the departure from the idealised curves, and the likely causes. We have also included regions like the Arabian examples, where there are good fits between the forward modelled and backstripped curves, but the potential tectonic overprints to the lithosphere thickness make comparisons unviable. The modelled curves are never going to flatten completely, but each of the examples we've used is now 100s of millions of years after basin initiation, and would not be expected to subside much more.

5. Details of the backstripping process should be provided (sediment densities, porosity, etc. and whether these properties were varied between the regions). More importantly, it seems that some subsidence curves come from published literature (pg 4, line ~46). Was the backstripping to get these curves done in a manner that is consistent with this study?

#There's now an account of the parameters: we followed the compaction relationships of Sclater and Christie (1980), which should be appropriate because they were derived for siliciclastic successions, like the majority of the stratigraphy we consider. A global eustatic sea-level curve (Haq and Schutter, 2008) is used to remove the effects of sea-level changes. Yes, the backstripping of the curves from S. Arica was carried out parallel to this study, in a manner consistent with ours.

6. The proposed subsidence model bears some similarities to the cooling model that has been proposed for orogenic regions (e.g., Fischer, 'Waning buoyancy in the crustal roots of old mountains', Nature, v. 417, p. 933-936, 2002; Hyndman et al., 'Subduction zone backarcs, mobile belts and orogenic heat', GSA Today, v. 15(2), p. 4-10, 2005). The difference is that these studies focus on high elevation regions, whereas the current study focuses on the basins. These studies should be referenced.

#References added. The Hyndman et al paper also supports our introductory material that juvenile accretionary orogens tend to be underlain by thin lithosphere; see their figures 5 and 8 for example.

7. As the lithosphere cools, it will become gravitationally unstable, but it is assumed that this lithosphere remains intact, which allows it to continue to thicken after the onset of cooling. It would be useful to state this and provide some discussion about what would be needed to prevent gravitational removal of this material.

#Although we do not explicitly model any gravitational instabilities, we are using a plate model instead of the halfspace cooling model. Therefore, we do account for the reduced thickening that any lithospheric instabilities cause, in a similar way as originally proposed for oceanic lithosphere (Parsons and Sclater, 1977). This is now made more explicitly in the methodology description.

8. pg 4, lines ~5-21: The last two paragraphs of the Introduction seem a little out of place. In particular, it isn't clear how the second-last paragraph justifies the need for a new mechanism for lithosphere evolution.

#The final paragraph of the Introduction has now been moved to the start of section 3, and modified. The second-last paragraph has been extended, and makes the case that none of the conventional models of rifting, foreland basin flexure or post-rift subsidence fit the vast dimensions or geometries of the basins we describe (picking on the North Africa-Arabia example).

9. pg 17, line ~35: either a reference is needed or there should be a more detailed discussion about why a flexural model will not fit the subsidence.

#Both a reference and a short explanation are added at this point.

10. Figure 5 - the left plot cools to 122 km final thickness, but the right plot cools to 139 km final thickness. What mechanism would cause the difference in lithosphere thickness? The final

lithosphere thickness also varies for Eastern Australia (Fig 7). (this may be related to the confusion about what time corresponds to the final thickness)

#We have pointed out in the manuscript that the models are run with varying final lithosphere thickness, until a good fit is made to the backstripped data. The value used in the forward model run is then compared with geophysical data for the lithosphere thickness. In each case where such data are available and clear-cut there is good agreement. But, unfortunately Arabia is not appropriate to include in these comparisons, because of two reasons. First, there is the potential overprinting by the more recent collision to the north and plume/ocean spreading to the south and west. Second, papers on the lithospheric thickness are different for the same areas of the Arabian Plate (references now added to the paper), and it is not clear which story, if either, is right. What we have done is add a note that there is no simple geological explanation we are aware of why the lithosphere thickness should vary as it does between the two sites in Fig. 5, but that it thins in the direction noted by Hansen et al (2007).

11. Figures 3-7 - it would be helpful if the individual plots were labeled a, b, etc., so that they could be directly referenced in the text. In places it is hard to relate the main text with individual figures. For example: does 'Cape 1' in Fig 4 belong to the Cape-Karoo Basin or the Cape Fold Belt discussed on pg 15?

#Done.

Reviewer #2: This paper presents additional support for a new basin formation mechanism for accretionary orogens introduced by Holt et al (2010). The paper describes 18 stratigraphic sections and related tectonic subsidence curves from five different sedimentary basins around the globe located on juvenile crust generated by accretionary orogens.

The shape of the subsidence curves resembles the "classic" subsidence curve for extensional rifted margins, however without the initial rapid syn-rift phase. The shape of the subsidence curves, therefore, is consistently similar to the post-extensional cooling branch of "classic" subsidence curves.

Using a numerical forward model for the new basin formation mechanism, the authors demonstrate that this consistent shape can be explained by thermal subsidence of a crust with normal thickness, but low initial thickness of the mantle lithosphere. The authors argue that such a configuration (i.e. normal crust, thinned mantle lithosphere) is typical for lithosphere created during formation of accretionary orogens.

Main comments

This paper is a follow up of the paper by Holt et al. (2010), in which a new basin formation mechanism for accretionary orogens is introduced and described in detail, including supporting evidence by wells from two sedimentary basins. The current paper provides additional support for this new basin formation mechanism by presenting results from backstripping analyses and forward modelling of a number of stratigraphic sections in another five sedimentary basins around the globe.

The presented analysis is sound and the results to my opinion indeed support the new basin formation mechanism. It, therefore, is important to publish these results. However, the paper would benefit by a more detailed description of the new basin formation mechanism for accretionary orogens presented by Holt et al (2010) to better assess and appreciate the new, additional evidence presented in this paper. This will strengthen the paper to become a truly stand-alone paper, without the need to also have to read the paper by Holt et al. (2010).

#There is now more text explaining the origin of the basins, in the Introduction.

Paper is well written, good structured. Figures are clear and support the main text. Description of the stratigraphic sections and sedimentary basins is in sufficient detail. Perhaps add for each basin a chrono-stratigraphic column (including phases of uplift and/or subsidence) as a graphical representation/summary of the detailed textual description?

#We have not acted on this suggestion, because we took care to provide detailed accounts and references of the geological columns used, in our text. This includes data about the lithologies, water depths, uncertainties and caveats, which are hard to capture in simple summary columns.

Fred Beekman

Department of Earth Sciences, Utrecht University September 2014.

***Highlights**

Highlights

- We propose that thermal subsidence can explain sedimentary basins on accretionary crust
- We present backstripped subsidence curves from five sedimentary basins worldwide
- Backstripped subsidence curves match forward modelling of thermal subsidence
- Our model does not need late stage orogenic extension or lithosphere delamination

*Revised manuscript with changes marked

Basin formation by thermal subsidence of accretionary orogens

P.J. Holt, M.B. Allen* and J. van Hunen

Department of Earth Sciences, University of Durham, Durham, DH1 3LE, UK

***tel: +44 (0)191 3342344; fax: +44 (0)191 3342301; e-mail: m.b.allen@durham.ac.uk**

Abstract

Subsidence patterns of 18 stratigraphic sections from five sedimentary basins around the world are analysed by forward and inverse modelling, in order to explain the mechanisms by which basins form on the juvenile crust generated by accretionary orogens. Study areas are the Paraná Basin (Brazil), Karoo Basin and Cape Fold Belt (South Africa), the Arabian Platform, Scythian and Turan platforms (Central Asia) and eastern Australia. The form of the tectonic subsidence curves derived from backstripping analysis is consistent with results from a forward model, which produces thermal subsidence of crust with normal thickness (~35 km) but low initial mantle lithosphere thickness. This high thickness ratio of crust:mantle lithosphere is the plausible initial configuration of lithosphere produced by accretionary tectonics. Our results do not require late stage orogenic extension or lithosphere delamination as a precursor to the thermal subsidence phase.

Keywords: basin; accretionary crust; thermal subsidence; juvenile

1. Introduction

The subsidence mechanism of intercratonic (intracontinental, or simply cratonic) basins has long been debated. These broad, uniform, basins are not easily explained by either rifting or lithospheric flexure (Allen and Allen, 2005). Holt et al (2010) studied the Ghadames and Kufra basins, North Africa, and suggested that their Palaeozoic subsidence was a consequence of the formational properties of the region's Neoproterozoic accretionary crust (Bumby and Guiraud, 2005; Caby and Monié, 2003; Guiraud and Bosworth, 1999). Such crust inherits the thin mantle lithosphere of many of its constituent building blocks (island arcs, accretionary wedges and young oceanic crust), and as this cools and thickens following tectonic assembly it causes subsidence as an isostatic response. However, it has not yet been proven if the process is an inherent property of juvenile crust generated by accretionary orogeny (Cawood et al., 2009), and therefore generally applicable. This paper aims to test this subsidence mechanism by looking at an overview of the subsidence patterns from a number of regions of accretionary crust.

Accretionary crust is defined as continental crust which forms during an accretionary orogen, which unlike a collisional orogen overlies at least one active oceanic subduction zone throughout its history (e.g. Şengör and Natal'in, 1996; Xiao et al., 2004; Collins et al., 2011; Kusky et al., 2013). It may also be referred to as juvenile crust (in relation to older cratonic crust). Accretionary orogens occur on the margins of a pre-existing continental nuclei, and are a focus for crustal growth. For example, the majority of granitoids from the Central Asian Orogenic Belt consist of high proportions (60 to 100%) of mantle-derived material (Jahn, 2000). Accretionary crust can vary in thickness from <30 km to >50 km. It is made up of differing terranes including island arcs, slivers of back arc crust, accretionary wedges from the forearc, slices of obducted oceanic crust and older microcontinental blocks embedded in broad collages of more juvenile material.

A key aspect of such crust is that it may be of near normal thickness, but is commonly underlain by thin mantle lithosphere at the time of accretion (e.g. Zhao et al., 1994; Zor et al., 2003). The reason for this is that the tectonic and magmatic processes that produce such crust are not necessarily complemented by equivalent processes to form an underlying mantle lithosphere. For example, slivers of a subducting plate may be scraped-off and accumulate to form an accretionary wedge above the subduction zone, but this is a process that builds crust, not mantle lithosphere. Also, before final accretion and the end of subduction, corner flow of the hydrated, weak mantle wedge may act to limit and reduce mantle lithosphere thickness (e.g. Eberle et al., 2002; Hyndman et al., 2005). Once final subduction has ceased under an accretionary orogeny, any such thin mantle lithosphere will tend to thicken, in the manner of lithosphere thinned after a rifting event (McKenzie, 1978), with the crucial difference that there need not have been any such stretching event to produce the thin mantle lithosphere.

Ultimately, such accretionary orogens may be the principal sites for net crustal growth, and have operated as such back into the Archaean (Cawood et al., 2009). The ages of accretion for the continental crust are shown in Fig. 1. Dimensions may be vast: 1000s x 1000s of km.

Many of these accretionary orogens have large, intact, platformal sedimentary sequences that accumulated upon them. This study examines the Paraná Basin, Cape Fold Belt and Karoo Basin, Arabian Platform, Scythian and Turan platforms and the post-Tasmanide basins of eastern Australia. These areas represent basins established over accretionary crust that formed at various times ranging from the Neoproterozoic to the Mesozoic. The global spread of the study areas gives confidence that we are dealing with a fundamental process, rather than a localised phenomenon. Basins were chosen because they are large, representative features for which data are available; there was no filtering of locations to try and find the best fits to the proposed model.

A number of other subsidence mechanisms have been suggested for these basins. Recently, it was suggested that many such basins form due to stretching of the continental lithosphere at low strain rates for long periods of time (50 – 100 Myrs) (Armitage and Allen, 2010). This produces a subsidence profile that begins with a straight line during the stretching phase, and then has a slight kink followed by a curved section caused by cooling acting over the stretched area. Dynamic topography has been suggested as an appropriate basin-forming mechanism (e.g. Gurnis, 1992), whereby subsidence is related to large-scale mantle flow patterns. It has also been suggested that regional subsidence is due to orogenic collapse following an accretionary orogeny, because the mantle lithosphere undergoes delamination (Ashwal and Burke, 1989, Burke et al., 2003). This scenario envisions a high density of small rifts, similar to the Basin and Range province, followed by a period of broad scale uniform subsidence with an exponential decay as the delaminated lithosphere is replaced by cooling upper mantle. Avigad and Gvirtzman (2009) suggested that there was partial mantle lithosphere detachment under the Arabian region in the Late Proterozoic, leading to initial surface uplift, but subsequent cooling and subsidence. There are similarities between this model and our study (in that both models envisage thermal subsidence as thin lithosphere cools and thickens), but we do not require the initial detachment.

There are many other mechanisms which have been suggested for individual basins, such as simple rifting (Oliveira and Mohriak, 2003) or back arc extension (Thomas et al., 1999), and flexure to create a foreland basin (Catuneanu, 2004; Milani and De Wit, 2008). We propose that the large scale and geometry of each of the basins in this study are incompatible with these “conventional” mechanisms. For example, the Palaeozoic basins of North Africa and Arabia represent an original “megabasin” covering ~10,000,000 km^2 from the Atlantic margin to the eastern edge of Arabia. Allowing for continental fragments now dispersed within Iran and adjacent countries, it was probably once even larger (Şengör and Natal’in, 2006).

2. Methodology

The first step in assessing the cause of the subsidence in each region is to backstrip the sedimentary record to get the tectonic subsidence of the region, i.e. inverse modelling. Results can then be compared to subsidence produced by a numerical forward model of thickening and cooling of the mantle lithosphere.

Backstripping is the process of calculating the tectonic subsidence from a sedimentary column. The practice is commonplace and the approach used here follows that of Watts and Ryan (1976), described in detail in Holt et al. (2010). We use standard relationships from published work (Sclater and Christie, 1980) for the porosity-depth relationships. A global eustatic sea-level curve (Haq and Schutter, 2008) is used to remove the effects of sea-level changes. Some of the study areas already have backstripped subsidence curves available in the literature. In other areas backstripping was carried out using available published records of the stratigraphy, either from well data, regional cross-sections constructed using seismic data, or regional stratigraphic columns based on thicknesses from fieldwork studies. In each region different data sources are used if available, to allow comparison between subsidence curves calculated from different data sets. Where there is disagreement in the literature as to the ages of the sediments, a subsidence curve is calculated for each conflicting interpretation.

The subsidence produced by thickening and cooling of the lithosphere beneath accretionary crust is calculated using a numerical forward model described in Holt et al. (2010), and explained below. This model calculates the conductive heat flow through a column of crust and upper mantle material and then the resultant subsidence of the column. The subsidence calculated is water loaded tectonic subsidence and therefore is directly comparable to that calculated from the backstripping.

The numerical subsidence model is based on and tested against the plate models for sea floor spreading (Parsons and Sclater, 1977). It is modified to include layered continental crust with radioactive heat production. It solves the vertical conductive heat flow through a one-dimensional column of the lithosphere and upper mantle:

$$\rho C_p \frac{\partial T}{\partial t} = \frac{\partial}{\partial z}(k \frac{\partial T}{\partial z}) + A \quad (1)$$

Equation 1 is solved using a finite difference technique with a grid resolution of 1 km. *T* is the temperature of the rock at a particular point in the grid at depth *z*. *A* is the contribution of radioactive heat production and *t* is the time over which the temperature is changing. Time-stepping is performed with an forward Euler time-integration scheme. The material properties of the rock are the thermal conductivity (*k)*, the specific heat capacity (C_p) and the density (ρ). The density of the rock is dependant on the temperature and is calculated using equation 2.

$$\rho = \rho_0(1 - \alpha(T - T_0)) \quad (2)$$

In Equation 2 the reference density (ρ_0) and the coefficient of thermal expansion (α) are dependent on the rock type. The values used for all the parameters in Equations 1 and 2 follow Holt et al. (2010).

The model has a felsic upper crust and granulitic lower crust, which is underlain by mantle lithosphere. The base of the lithosphere is purely thermal rather than compositional and is defined by the temperature below which the mantle rock does not deform significantly over geological timescales. The 1200 °C isotherm is used (Turcotte and Schubert, 2002). The model starts with a 20 km thick mantle lithosphere, to represent the initial thin mantle lithosphere typical of accretionary orogens at the time of their formation. The temperature at the surface of the model is set as 0°C. The temperature at the base of the model is calculated using the potential temperature (i.e. a given mantle temperature extrapolated to the surface) and an adiabatic gradient of 0.3°C per km. Constant temperature boundary conditions are used at the top and bottom of the model. The initial temperature conditions follow this mantle adiabat to

up to a transition point 20 km below the crust above which they follow a linear gradient to the surface. The depth and therefore temperature at this transition point is dependent on the thickness of the crust and the potential temperature for the surface. The elevation is calibrated from the density profile of the column using a column of hot mid ocean ridge material with a 7 km thick basaltic-gabbroic crust at 3 km below sea-level as reference. Standard Pratt isostasy is used. When the topography of the model drops below sea level the basin is filled with water. The thermal boundary condition is applied to the basement floor because water in the basin would have an almost uniform temperature due to convection. However, the water is included in the isostacy so the model effectively produces water loaded tectonic subsidence.

One inherent weakness of the plate model is that it only calculates the heat transfer by conduction (Parsons and Sclater, 1977). At the base of the plate heat transfer changes from conduction to convection (e.g. van Hunen et al., 2005). The plate model does not explicitly describe the physics of this transition, but provides a good fit to the bathymetry and heatflow data (Huang and Zhong, 2005). Gravitational instabilities of the thickening lithosphere are not explicitly included in our model, but the average reduction in lithospheric thickening of any detaching or delaminating lithosphere is accounted for by the plate model.

We ignore the temperature dependence of k, C_p and α. This assumption slightly overestimates temperatures in the top half of the model and underestimates temperatures in the bottom half of the model (McKenzie et al., 2005). This means the depth to the base of the lithosphere is an upper limit. We do not model metamorphic reactions in the cooling lithosphere (Fischer, 2002).

The modelled subsidence is most sensitive to variations in the thickness of the crust and the final thickness of the lithosphere, which is controlled by the model thickness (plate thickness) (Holt et al., 2010). Therefore these two parameters are varied to find the column of lithosphere and crust which best fits the observed subsidence for each region, as represented

by the backstripped subsidence curves. Other parameters are kept constant between the different models. The best crust and lithosphere thickness values produced by the forward modelling are compared to published measurements of the crustal and lithospheric thickness, to see if model values are realistic. There is a caveat here that we have to use present day thickness values, leaving it possible that these have changed since the end of basin formation, which was 100s of millions of years ago in some of the examples we study. To minimise this effect we have used basins and sections from regions that have not been heavily overprinted by later tectonic events, although departures from idealised behaviour are present in some of the curves, and are discussed individually in the Results section.

3. Regional geology

Each region is looked at in turn in this section, considering both the accretion history of the area and the basins formed on the juvenile crust. It is not the intention to review each region in exhaustive detail, rather the aim is to give an overview, and compare the subsidence across different regions in section 4.

3.1 South America: Paraná Basin

Much of western Brazil and Argentina are made up of crust accreted in the Brasiliano orogeny (Bumby and Guiraud, 2005). Before the formation of the Atlantic, this was a continuous band of accretionary crust that formed in the Late Proterozoic (Neves and Fuck, 2013). The assembly of the North African accretionary crust appears to have finished marginally earlier with the final phase of accretion occurring at ~600 Ma, dated using orogenic granites (Liégeois et al., 1994). Similar batholiths in the Brasiliano collage formed between 590 and 500 Ma (Almeida et al., 2000). The crust is not exclusively made up of juvenile terranes, but includes numerous older Proterozoic and even some Archaean blocks (Brito Neves, 2002).

However, these are reworked during the orogeny and should not affect the initial conditions of a thin lithosphere suggested in the subsidence mechanism being tested.

There are a number of basins situated in this region, such as the Parnaíba Basin, the Paraná Basin and its extension into Argentina, the Choco-Paraná Basin, shown in Fig. 2a. The Paraná Basin is situated in southern Brazil and covers an area of over 2 million km^2 (Fig. 2a). The earliest sediments within it date from the late Ordovician, and the sedimentary succession continues through to the Jurassic where it is capped by lavas of the Serra Geral, which are related to rifting of the Atlantic margin. Detailed descriptions of the sedimentary fill are given in Zalán et al., (1990) and Eyles et al., (1993). The earliest strata are known as the Silurian sequence, although it starts with continental sandstones and conglomerates of Middle to Late Ordovician age (Zalán et al. (1990) and Eyles et al. (1993) disagree as to exactly when deposition started).

These rocks change gradationally into shales and siltstones of Silurian age, and to shallow marine sandstones by the end of the Silurian. There was a period of erosion during the Early Devonian, followed by deposition of the Devonian sequence. Again, this shows a complete transgressive – regressive cycle, beginning with transgressive sandstones, fining up into marine shales, which are overlain by deltaic sandstones. This deposition was followed by another hiatus and further erosion, which lasted for much of the Carboniferous. Sedimentation began again with continental redbeds at ~ 270 Ma, followed by deposition of glacial marine sediments and another transgressive – regressive cycle during the Permian. There is some disagreement between different authors. Eyles et al., (1993) showed continuous sedimentation through to the base of the Serra Geral lavas, whereas Zalán et al., (1990) reported a hiatus during the Lopingian (end Permian) and Early Triassic. Both sets of authors agree the overlying Triassic sediments are entirely continental, consisting of lacustrine, fluvial

and aeolian sediments that continue into the Jurassic. Jurassic strata are interbedded with the Serra Geral lavas.

3.2 Southern Africa: Cape Fold Belt and the Karoo Basin

The Cape Fold Belt and the Karoo Basin in southern Africa (Fig. 2b) have similar sedimentary fills to the Paraná Basin described above. The subsidence patterns are also similar, leading to a number of correlations being suggested (Milani and De Wit, 2008). However, unlike South America the African regions are not entirely underlain by accretionary crust (Fig. 1). The Cape Fold Belt is largely underlain by Neoproterozoic accretionary crust of the Damara Belt, which forms part of the same mobile belt as the South American accretionary crust. The Cape-Karoo Basin to the north is underlain by Mesoproterozoic basement, and its western side is floored by Archaean basement of the Kaapvaal craton (Milani and De Wit, 2008). If the subsidence mechanism suggested also formed the Cape-Karoo Basin then the older crust must have been remobilised by the Pan African orogeny. This is supported by evidence from the Mesoproterozoic basement flanking the Damara belt which has been rejuvenated (Frimmel and Frank, 1998). Also the basement of the combined Cape-Karoo Basin is intruded by Cambrian A-type granites indicating involvement in the accretion process (Milani and De Wit, 2008). A similar situation is seen in the North African accretionary crust, where there is evidence for reworking of a Palaeoproterozoic cratonic block during the Pan African, and the existence of the older crust has no discernible effect on the subsidence patterns (Abdelsalam et al., 2002).

This pattern suggests that the crustal accretion processes of juvenile orogens can lead to tectonic reactivation and thinning of neighbouring lithosphere. This effect could be because during the accretion there is an intervening ocean subducting beneath the older crust, and the

subduction process leads to thinning the older lithosphere through corner flow or back arc stretching (Arcay et al., 2006; van Keken, 2003). Sedimentation in both the Cape Fold Belt and the Cape-Karoo Basin began with a succession of mature, continental-derived, siliciclastic sediments. Deposition began sometime in the mid Cambrian, although this timing is difficult to date, and continued until the Devonian. Strata show glacial influence during the Ordovician, followed by shales that represent maximum flooding of the Ordovician to Silurian transgressive – regressive cycle (Turner et al., 2011). Unlike the Paraná Basin, there is no significant hiatus before the Devonian cycle. The sedimentation is similar in character to the Paraná, showing a transgressive – regressive cycle with silt and mudstones representing the maximum flooding, which shallow upwards to Early Carboniferous lacustrine sediments. These Carboniferous strata are the youngest preserved sedimentary rocks in the Cape Fold Belt (Turner et al., 2011).

In the Cape-Karoo Basin the Carboniferous lacustrine rocks are overlain by glaciogenic sediments made up of diamictites and rhythmites, which continued until the Early Permian. These strata are succeeded by black mudstones, grading into deltaic sands. There is some debate as to whether the glaciogenic sediments and those following are deposited into a marine or lacustrine environment (Milani and De Wit, 2008). At the end Permian there is a deepening of the basin as black shale is deposited. There is then a gradual shallowing evidenced by distal turbidites passing upwards into coarser turbidites and ultimately shoreline and fluvial deposits. From this point on the sediments are terrestrial, represented by desertification throughout the Triassic. The sequence is terminated by the eruption of the Karoo Large Igneous Province in the Jurassic. A more detailed overview of the sedimentary history of the Cape Fold Belt can be found in Turner et al., (2011) and for the Cape-Karoo Basin in Milani and De Wit, (2008).

3.3 Arabia

The Arabian crust also forms part of the accretionary crust formed during the Pan African orogeny, and was contiguous with counterparts in North Africa before the opening of the Red Sea. Proterozoic basement is particularly well exposed along the flanks of the Red Sea due to Cenozoic surface uplift at the margins of that rift zone. Therefore the region provides good insight into the makeup and assembly process of accretionary crust. The Arabian crust is composed of numerous sutured terranes. Many of these terranes are island arcs, dated between 870 – 690 Ma (Stern, 1994). There are also ophiolitic terranes, accretionary wedges (not to be confused with accretionary crust) and older terranes from the Meso-Palaeoproterozoic. In his area of study Stern, (1994) described roughly two thirds of the crust as juvenile. The geochemistry of xenoliths brought up from the lower crust and mantle by Miocene and younger volcanics in Syria, Jordan and Saudi Arabia confirms that regions with sedimentary cover are also underlain by juvenile basement, made up of Neoproterozoic island arc terranes (Al-Mishwat and Nasir, 2004). The accretion was a gradual process with some terranes colliding with each other to form composite terranes, before colliding in the main accretionary orogen. The date of the final phase of accretion is ~550 Ma in the east of Arabia, but gets progressively younger westwards, and is ~500 Ma on the flank of the Red Sea (Stern, 1994).

Apart from where the basement is exposed alongside the Red Sea most of Arabia is blanketed by Palaeozoic sediments (Konert et al., 2001), as shown in Fig. 2c, which collectively form the Arabian Platform. The earliest sediments are continental clastics which are Cambrian in age. These were deposited in the north and east, but are not seen in the southwest of Arabia. During the Ordovician the marine influence spread inland, and the area of deposition expanded to the southwest. Even so, Early Ordovician sediments are mostly sandstones except along the fringes of the platform. These were overlain by fine grained clastics in the Mid Ordovician. The Late Ordovician saw a period of glaciation with widespread erosion inland and glaciogenic deposition near the edges of the platform. This was followed by filling of the glacial

topography with coarse clastics and then a widespread transgression during the Silurian. In the Early Silurian shales were deposited, which are an important source rock for hydrocarbons in some areas. The sediments then record the transgressive phase of the cycle coarsening upwards into shoreface and deltaic sandstones. More detail is available in Garfunkel (2002), who notes that the same sedimentary patterns are seen across much of North Africa and therefore concludes that it formed a 2000 km wide platform. As Fig. 2c shows, later sediments are not as well preserved and have a patchier distribution.

There was then a hiatus in sedimentation, which resumed in the Middle Silurian in central Arabia (McGillivray and Husseini, 1992), but did not begin until the Late Silurian further north in Syria (Best et al., 1993) or Iraq (Al-Juboury and Al-Hadidy, 2009). This hiatus was related to the "Caledonian orogeny", which is seen across North Africa as well. The quotation marks are advisable: this deformation is Early Palaeozoic in age, and for this reason commonly termed "Caledonian", but there is no simple correlation with the orogeny of that name in northwest Europe and conjugate parts of North America.

Sedimentation renewed in the Devonian in central Arabia, with a transgressive to regressive cycle that began with fluvial sediments. These rocks pass into marine sandstones with minor carbonates in the Emsian, then back into shoreface sandstones. In the north of the platform the hiatus lasted until the end of the Mid Devonian. The sequence deposited afterwards is mainly siltstones and shales, with some sandstones and minor carbonates, and the youngest rocks are from the end of the Mississippian. In both areas the top of the sediments is marked by an erosional surface referred to as the Hercynian event – with a similar caveat about the use of this term to "Caledonian". This has cut down to the Silurian sediments in some areas, so extensive section may be missing. Both areas experience subsequent phases of subsidence. However the modelling results suggest that the effect of cooling and thickening of lithosphere should be negligible by this point (> 200 Myrs after accretion has finished).

Therefore subsequent episodes of subsidence are likely to be caused by other mechanisms. This illustrates the polyphase nature of many of these basins. In Arabia, the later phases are much better studied because they host the majority of the discovered hydrocarbons (Guiraud and Bosworth, 1999).

3.4 Scythia and Turan

The platforms of Scythia and Turan (Fig. 2d) formed upon a band of accretionary crust which developed on the northern side of the Palaeo-Tethys Ocean (Fig. 1). The region is unique in this study, in that it did not lie on the margin of Gondwana. The Middle Caspian Basin lies between the Scythian and Turan platforms. The evolution of both the basement and cover of the Middle Caspian Basin probably resembles that of the adjacent areas, but as there are fewer details known it is not analysed here.

Assembly of the Scythian and Turan basement was largely a late Palaeozoic process (Şengör and Natal'in, 1996). The regional basement is penetrated by wells (Fig. 2d) that encountered a mixture of granitoids, mafic, felsic and intermediate volcanics of Carboniferous to Triassic age. Available geochemical data show a subduction-related origin for these rocks. The terranes which make up the basement are interpreted as originating mostly as paired forearc and arc units (Natal'in and Şengör, 2005). Amalgamation finished during the mid-Triassic in Turan.

Initial platform sediments overlap in age with the final phase of accretion. Sedimentation began on the Turan Platform in the Permian with continental sediments. The platform was then submerged, and sedimentation switched to marine clastics which continued into the Triassic. Thomas et al. (1999) note the main extension phase is Late Permian – Early

Triassic, interpreted to be caused by back-arc stretching. During the Late Triassic there was a period of compression, with some erosion in the north.

The earliest sedimentation on the Scythian Platform is Early Triassic in age. There are a number of north-south trending rifts (Nikishin et al., 2001). During the Late Triassic – Early Jurassic there was compression, as the Alborz terrane collided to the south during the closure of Palaeo-Tethys. This led to erosion, which obscures the original extent of the Triassic strata. The Scythian Platform remained above sea-level during the Early Jurassic. In the Middle Jurassic the east of the platform was flooded and a clastic sequence was deposited. The western side of the platform remained above sea-level. On the Turan Platform, the Early Jurassic sediments to the north and east were fluvial and deltaic, whereas in the southwest shallow marine sandstones fined upwards into silts and shales. These patterns were repeated in the Late Jurassic where a regression caused evaporites to be deposited to the north and east, while in the southwest carbonates were deposited. There was major transgression across the whole platform during the Cretaceous (Thomas et al., 1999), and marine sediments were deposited, including chalk.

There was gentle folding during the Early Paleocene before sedimentation resumed across the combined platform. Shallow marine sediments were deposited during the rest of the Paleocene and the Eocene. Sedimentation terminated across much of the Scythian Platform during the Eocene. In Turan there was a pulse of Oligocene to Quaternary subsidence caused by the collision between Arabia and Eurasia. The sediments deposited at this time are clastics shed from the rising mountains to the south.

3.5 Eastern Australia

The Tasmanides of eastern Australia were accreted from the Mid Cambrian to the Permian (Fig. 2e), a similar time scale to the accretionary crust in Arabia and North Africa.

There is a mix of terrane types including older Proterozoic crustal fragments, island arcs, accretionary complexes and ophiolitic terranes: a thorough review is provided by Glen (2005) and Veevers (2006), from which this summary is taken. Accretionary crust formed over five distinct orogens, which are marked by a period of collision of new terranes onto the margin. The collisional phase was followed by a period of extension while subduction continued along the margin of the region. This process indicates that the lithosphere remained thin until the accretion terminated, because it was being stretched after each collision phase. The earlier orogens were originally thought to contain a greater proportion of older crust, but this has been recently revised based on dating of basement from new wells (Glen, 2005; 2013). Many Proterozoic microcontinents were rejuvenated during accretion and were intruded by granitoids.

Much of the Tasmanides (10^6 km^2) are covered by platformal Mesozoic to Cenozoic sedimentary cover (Fig. 2e). The evolution of the platform is described in Gallagher et al. (1994). The earliest platform sediments are Early Permian in age. They are found in the Eromanga and Cooper basins in the west of the Tasmanides, and the Bowen-Surat-Sydney Basin, which trends north-south in the east of the region. These sediments are shallow marine clastics in the east and continental clastics (fluvial and lacustrine sediments) in the west. In the Mid Permian sedimentation ceased and there was a brief period of erosion across the platform before continental clastics were deposited during the Triassic. During the Late Triassic there was another period of erosion, which was more severe towards the east. In the Jurassic a fining-upwards succession passing from coarse sandstones to shales was deposited across the entire platform and is interpreted to be a fluvial environment, changing upwards into a lacustrine environment. The sediments contain progressively more volcanically derived material in the east suggesting there was a volcanic margin to the east of the platform. In the Early Cretaceous the basins were connected to the sea and sediments fluctuate between shallow marine and deltaic sediments in both the Eromanga and Surat basins. There was a

regression in the east around 110 Ma , and during the Cenomanian continental sediments were deposited. In the west there is a brief period of increased subsidence at 100 Ma. Sedimentation ceased shortly afterwards.

4. Results

4.1. South America

Backstripped curves for the Paraná Basin and PreCordillera were published by Milani and De Wit (2008). Published stratigraphy was also used to generate the backstripped curves in Fig. 3 alongside the best-fitting forward model curve. A pseudo-well from a cross-section through the Paraná Basin (Zalán et al., 1990) was backstripped as well, with both of the conflicting age estimates for the sediments (Eyles et al., 1993; Zalán et al., 1990).

When the backstripped curves are compared to the forward model, the first 150 Myrs shows subsidence similar to a modelled curve produced with a 36 km thick crust and a final lithospheric thickness of 130 km. Note that in Fig. 3 and subsequent similar figures, the initial part of the forward modelling curve, where the elevation was above sea level, is not shown. This represents a time of up to several 10s of millions of years and 100s of metres of subsidence that are not regionally recorded in the sedimentary record.

The fit between the backstripped and forward modelled curves is not perfect, in part because there are periods of uplift and erosion, which are evident in the backstripping, but not the forward modelling. After 310 Ma there is sudden increase in the subsidence rates. This coincides with collision of the Gondwanides along the western margin of South America. It has been suggested the Paraná Basin became a foreland basin at this time, causing renewed

subsidence (Milani and De Wit, 2008). The subsidence in the PreCordillera began ~100 Ma earlier and may reflect earlier accretion and cratonisation of the crust beneath this basin before it docked with the rest of South America. This collision at the end of the Ordovician could explain the increased subsidence observed after 400 Ma (Milani and De Wit, 2008). It is fitted best by a model with a 30 km thick crust and a 130 km thick lithosphere. The fit to the model is very close for the first 150 Ma. The results show that lithospheric cooling of accretionary crust can explain the overall subsidence seen in the basins in this region of South America, before a later phase of subsidence due to flexure in a foreland basin setting. The crustal thickness used for both basins is consistent with the results of Feng et al., (2007) who measure the Moho varying between 35 and 40 km depth beneath Paraná, and between 25 and 35 km depth beneath the PreCordillera. Lithosphere thickness is not well constrained.

4.2 South Africa

The subsidence curves for the Cape-Karoo Basin are from data in Cloetingh et al., (1992) and the curve for the Cape Fold Belt is from outcrop data in Turner et al., (2011). All these data are composite thicknesses from regional stratigraphy. Both subsidence curves for the Cape-Karoo Basin are fitted well by a forward model with an initial crustal thickness of 27 km and a final lithospheric thickness of 122 km (Fig. 4). The subsidence of the Cape Fold Belt is matched most closely by an initial 23 km thick crust and a final 122 km thick lithosphere. However, to achieve this match an unusually thin initial lithosphere of only 27 km thickness is required. If a thicker initial lithosphere was used the shape of the curve would remain the same, but the first part of it would be missing as the crust would start below sea-level.

The crustal thickness values are in agreement with present crustal thickness, which thins towards the south from ~30 km to 25 km (Pasyanos and Nyblade, 2007). The regional best fitting lithospheric thickness is also in good agreement with the lithospheric thickness measured using shear wave tomography, which is ~120 km (Priestley and McKenzie, 2006).

Therefore the model provides a good fit to the subsidence curves in South Africa using parameters which match those published in the literature, notwishstanding that this is an area that may have been affected by both compressional deformation and magmatism/extension related to the opening of the South Atlantic. Similar to South America there is a phase of renewed subsidence, which has again been attributed to growth of the Gondwanides (Milani and De Wit, 2008).

4.3 Arabia

McGillivray and Husseini, (1992) published a number of wells through the Palaeozoic section in Syria. Of these, two penetrate crystalline basement and one finishes in the Cambrian, however all three are missing sections from the Devonian and Early Mississippian. The most complete in terms of sedimentary units is the Khanaser #1 well, which is therefore used in this study (Fig. 5). Published well data from central Arabia are sparser, therefore thicknesses from outcrop have been used instead (Best et al., 1993). Fig. 5 shows the fit of the modelled subsidence to the backstripping. The outcrop data from central Arabia is fitted best by a 33 km thick crust with a 139 km final lithospheric thickness. The model parameters used to acquire the best fit for the Khanaser #1 well are a 30 km thick crust with 122 km thick lithosphere. When the sedimentary cover is added the crustal thicknesses are both broadly in agreement with the 38 km inferred by Al-Mishwat and Nasir (2004). The slightly thinner crust in the north would also provide a neat explanation for the earlier onset of sedimentation than in the south of the platform. It is not clear why there should be a difference in the best-fit final lithosphere thickness between these two regions, although it matches the thinning in a northwards direction noted by Hansen et al. (2007). Comparison to the present day lithospheric thickness is not viable because it has been affected by later events, such as the collision between Arabia and Asia in the north (Priestley and McKenzie, 2006) and the rifting of the Red Sea in the South West (Pasyanos, 2010). Published estimates for the lithosphere

thickness under Arabia vary markedly between different authors (Hansen et al., 2007; Park et al., 2008; Jimenez-Munt et al., 2012), making it difficult to compare our model results with observations.

For both the outcrop and the well the proposed subsidence mechanism provides a reasonable fit to the backstripping, but there is a lot more variance from the predicted subsidence curves taken from the modelling than in the other regions studied. This may be because of the greater amount of erosion experienced by these sections than other regions in this study. However, there is still a good temporal link between the accretion and the subsidence as well as a broad fit to the subsidence curves, despite the problems with erosion.

4.4 Scythia and Turan

Sedimentary thicknesses for the Turan platform are taken from Thomas et al. (1999). They created an isopach map of each layer using regional seismic data constrained by 500 wells. These were used by Thomas et al. (1999) to create a number of cross-sections across the platform, one of which was used to provide the inputs for the backstripping in this study. Four columns were backstripped from the cross-section to look at the difference across the platform (Fig. 6).

The fit between the forward model and backstripping are shown in Fig. 6. The deepest sequence in the Khiva depression is fitted very well by a 28 km thick crust and a 155 km thick final lithosphere. For the other three columns the fit is good except for the first point. As mentioned previously the first layer of sediment is not divided beyond Permian and Triassic, which has been followed in the backstripping. Therefore the timing for the start of subsidence has the greatest uncertainty. Equally the area was still being influenced by accretion and rifting until the mid-Triassic, which could also affect the poor fit to the start point. The other points fit well with lithospheric cooling with the reduced subsidence being explained by a slight increase

in the crustal thickness to 31 km in the east. This fits with the observations of Natal'in and Şengör, (2005) who note that the forearc terranes, which are floored by oceanic crust coincide with the deepest sedimentary cover. The lithosphere thickness was kept constant across the Turan platform and is within the range of variation suggested for the region (120-180 km) (Pasyanos, 2010; Priestley and McKenzie, 2006).

4.5 Eastern Australia

Mesozoic subsidence patterns in eastern Australia are consistent with the pattern produced by cooling of the lithosphere rather than flexure caused by a subduction zone. The subsidence patterns are similar for wells >1000 km apart, in the direction across strike from the trend of the underlying orogenic belts. Additionally, the individual curves do not have the convex-up shape characteristic of tectonic subsidence curves for foreland basins (Allen and Allen, 2005).The backstripped subsidence curves fit the subsidence from the forward model for most of the timespan.

The wells in Fig. 7 are ordered from west to east and the best fitting models show a trend of a thicker final lithosphere in the west (154 km – Walkandi 1; Fig. 7A) than the east (122 km – Arlington 1; Fig. 7E). This agrees with the trend seen in surface wave tomography (Fishwick et al., 2008). Their results suggest a lithosphere of 150-200 km in the west which is in good agreement with the results of this study, however they only have a ~100 km thick lithosphere in the east which is thinner than the 120 km used in the best fitting model. The crustal thicknesses used in the model also fit reasonably well with those measured. The Moho depth beneath the Eromanga Basin is between 36-40 km (38 km – Walkandi forward model) and 34-36 km beneath the Surat Basin (34 km – Red Cap 1, 32 km – Arlington 1 forward models) (Collins et al., 2003). While the modelled subsidence does not explain the increased subsidence rates seen in the Late Cretaceous it does provide a good fit up to this point.

5. Discussion

Holt et al., (2010) showed that cooling and thickening of the lithosphere provided a good fit to the subsidence of two North African basins in a specific case study. This paper provides further evidence supporting this subsidence mechanism, and shows it is likely to be an inherent property of accretionary crust on a global scale.

Several other mechanisms have been suggested to explain the formation of the basins in this study. Rifting in some form has been suggested for the basins in North Africa (Lüning et al., 1999), South America (Oliveira and Mohriak, 2003), Turan (Thomas et al., 1999) and Australia (Korsch et al., 1988). A typical scenario is that the basins represent thermal subsidence following a conventional phase of extension. In some of the study areas there are indeed rifts visible on seismic data in some of the basins, but, they are only detected locally (e.g. Nikishin et al., 2001). It is possible that other rifts have not yet been discovered. However, many of the basins in this study are producing hydrocarbons or are actively being explored and extensive seismic data exist, so it is unlikely this is the case.

The mechanism of 'slow rifting' involves stretching at low strain rates over a long period of time (Allen and Armitage, 2011; Armitage and Allen, 2010). This produces a subsidence pattern which is initially linear during the slow stretching phase, with a kink when stretching ceases, followed by a decaying curve due to the thermal relaxation phase. When the first points on a subsidence curve are poorly dated it is difficult to distinguish between this 'slow rift' mechanism and the model proposed in this paper. This is the case in South Africa and for the Turan platform. However, in Australia the dating is good enough to show that the subsidence profiles are curved throughout for wells Arlington 1 and Walkandi 1, without an initial linear, slow rift phase, but consistent with the exponential decay of a thermal subsidence curve. The composite well from the Ghadames Basin backstripped in Holt et al, (2010) also has good age resolution for the first data points and is curved throughout. The

caveat that applies to conventional rifting also applies to this slow rift mechanism: there is a lack of imaged rifts in the basins. Armitage and Allen (2010) argued that slow rifting may result in deformation being spread over numerous small faults, which is why they are not imaged. This does not agree with the results from analogue models of rifting which show that lower strain rates lead to increased localisation of strain on fewer large faults (Bellahsen et al., 2003). The same has been observed for active rifts such as the East African rift (Mazzarini et al., 2004).

Slow rifting also requires the basin to be under tension for long periods of time whereas many of the basins show periods of compression in their history. This does not present a problem for cooling and thickening of the lithosphere because it acts in the background and certain times in the basin's history may be influenced by compressional processes, but when these cease the subsidence will continue.

Dynamic topography has also been suggested as a mechanism for forming intracontinental basins of the type analysed here (e.g. Gurnis, 1992; Heine et al., 2008). This model invokes subsidence caused by mantle flow patterns, for example in eastern Australia (Gallaher et al., 1994; Gurnis et al., 1998; Matthews et al,. 2011), but there are problems with its application to the basins in this study. First, there is no obvious reason why mantle downwellings would produce basin subsidence patterns that so closely mimic the thermal subsidence histories found in global examples, i.e. a negative exponential decay. Second, many applications of dynamic topography invoke subduction initiation for the generation of subsidence (Gurnis, 1992), whereas the geological record indicates that basin development begins after subduction has ended under an area.

Avigad and Gvirtzman (2009) produced a model for the subsidence of the Arabian-Nubian Shield that involved thermal subsidence, following loss of the entire mantle lithosphere. For this model to have generic implications, all such intracontinental basins would likewise need to

follow catastrophic delamination. We know of no direct evidence that this has occurred; instead small-scale convection beneath young orogens may be a common process (Kaislaniemi et al., 2014), but not producing regional or even local subsidence.

6. Conclusions

This study worked from the hypothesis that accretionary crust begins with thin underlying mantle lithosphere, which is a property of its origin by processes that favour near-normal crustal thickness, but not the generation of a complementary mantle keel. Subsequent cooling and thickening of the mantle lithosphere causes subsidence as an isostatic response. This basin forming mechanism was shown to be a viable formation mechanism for the Palaeozoic basins of North Africa in Holt et al (2010), with good agreement between forward modelling and backstripped subsidence curves. The present paper shows that the modelled subsidence from this mechanism fits the observed subsidence patterns of basins formed upon accretionary crust from around the world, suggesting that the mechanism is generically applicable to such crust.

Acknowledgements

We thank Statoil for the funding of PJH's original PhD project, and H.M. Bjørnseth for his support. We thank Fred Beekman and an anonymous referee for their helpful and constructive reviews.

References

Abdelsalam, M.G., Liégeois, J.P., Stern, R.J., 2002. The Saharan metacraton. In: Fritz, H., Loizenbauer, J. (Eds.), 18th colloquium of African Geology Journal of African Earth Sciences. Graz Austria. Elsevier, pp. 119–136.

Al-Juboury, A. I., Al-Hadidy, A. H., 2009. Petrololgy and depositional evolution of the Paleozoic rock of Iraq. Marine and Petroleum Geology 26, 208-231.

Al-Mishwat, A. T., Nasir, S. J., 2004. Composition of the lower crust of the Arabian Plate: a xenolith perspective. Lithos 72, 45-72.

Allen, P.A., Allen, J., 2005. Basin Analysis: Principles and Applications. Oxford, Blackwell Publishing.

Allen, P., Armitage, J. J., 2011. Cratonic Basins, In: Busby, C. J., and Pérez, A. A., (Eds.), Tectonics of sedimentary basins: Recent Advances. Cambridge, Wiley-Blackwell Science, pp. 602-620.

Almeida, F. F. M. d., Brito Neves, B. B. d., Carneiro, C. D. R., 2000. The origin and evolution of the South American Platform. Earth Science Reviews 50, 77-111.

Arcay, D., Doin, M.-P., Tric, E., Bousquet, R., de Capitani, C., 2006. Overriding plate thinning in subduction zones. Localised convection induced by slab dehydration. Geochemistry Geophysics Geosystems 7, Q02007, doi: 10.1029/2005GC001061.

Armitage, J. J., Allen, P. A., 2010. Cratonic basins and the long-term subsidence history of continental interiors. Journal of the Geological Society of London 167, 61-70.

Ashwal, L. D., Burke, K., 1989. African lithospheric structure, volcanism and topography. Earth and Planetary Science Letters 96, 8-14.

Avigad, D., Gvirtzman, Z., 2009. Late Neoproterozoic rise and fall of the northern Arabian-Nubian shield: The role of lithospheric mantle delamination and subsequent thermal subsidence. Tectonophysics 477, 217-228.

Begg, G.C., Griffin, W.L., Natapov, L.M., O'Reilly, S.Y., Grand, S.P., O'Neill, C.J., Hronsky, J.M.A., Djomani, Y.P., Swain, C.J., Deen, T., Bowden, P., 2009. The lithospheric architecture of Africa: Seismic tomography, mantle petrology, and tectonic evolution. Geosphere 5, 23-50.

Bellahsen, N., Daniel, J.-M., Bollinger, L., Burov, E., 2003. Influence of viscous layers on the growth of normal faults; insights from experimental and numerical models. Journal of Structural Geology 25, 1471-1485.

Best, J. A., Barazangi, M., Al-Saad, D., Sawaf, T., Gebran, A., 1993. Continental margin evolution of the Northern Arabian platform in Syria. AAPG Bulletin 77, 173-193.

Brito Neves, B. B. d., 2002. Main stages of the development of the sedimentary basins of South America and their relationship with the tectonics of supercontinents. Gondwana Research 4, 175-196.

Bumby, A. J., Guiraud, R., 2005. The geodynamic setting of the Phanerozoic basins of North Africa. Journal of African Earth Sciences 43, 1-12.

Burke, K., MacGregor, D.S., Cameron, N.R., 2003. Africa's petroleum systems: four tectonic 'Aces' in the past 600 million years. In: Arthur, T., MacGregor, D.S., Cmeron, N.R. (Eds.) Petroleum Geology of Africa: New Themes and Developing Technologies, vol. 207, Special Publications. Geological Society, London, pp. 21-60.

Caby, R., Monié, P., 2003. Neoproterozoic subductions and differential exhumation of western Hoggar (southwest Algeria): new structural, petrological and geochronological evidence. Journal of African Earth Sciences 37, 269-293.

Canil, D., 2008. Canada's craton: A bottoms-up view. GSA Today 18, 4-10.

Catuneanu, O., 2004. Retroarc foreland systems - evolution through time. Journal of African Earth Sciences 38, 225-242.

Cawood, P.A., Kroner, A., Collins, W.J., Kusky, T.M., Mooney, W.D., Windley, B.F., 2009. Accretionary orogens through Earth history, In: Cawood, P.A., Kroner, A. (Eds.), Earth Accretionary Systems in Space and Time. Geological Society Publishing House, Bath, pp. 1-36.

Cloetingh, S. A. P. L., Lankreijer, A., de Wit, M. J., Martinez, I., 1992. Subsidence history analyses and forward modelling of the Cape and Karoo Supergroups, In: de Wit, M. J., Ransome, I. D., (Eds.), Inversion tectonics of the Cape Fold Belt, Karoo and Cretaceous basins of Southern Africa. Rotterdam, A. A. Balkema, pp. 239-248.

Collins, C. D. N., Drummond, B. J., Nicoll, M. G., 2003. Crustal thickness patterns in the Australian continent, In: Hills, R. R., Müller, R. D., (Eds.), Evolution and Dynamics of the Australian Plate, Volume 372. Boulder, Colarado, Geological Society of America Special Paper, pp. 121-128.

Collins, W.J., Belousova, E.A., Kemp, A.I.S., Murphy, J.B., 2011. Two contrasting Phanerozoic orogenic systems revealed by hafnium isotope data. Nature Geoscience 4, 333-337.

Debayle, E., Kennett, B.L.N., 2003. Surface-wave studies of the Australian region. In: Hillis, R.R., Müller, R.D., (Eds.), Evolution and Dynamics of the Australian Plate, vol. 372, Boulder, Geological Society of America Special Publications, p.25-40.

Eberle, M. A., Grasset, O., Sotin, C., 2002. A numerical study of the interaction between the mantle wedge, subducting slab, and overriding plate. Physics of the Earth and Planetary Interiors 134, 191-202.

Eyles, C. H., Eyles, N., Franca, A. B., 1993. Glaciation and tectonics in an active intracratonic basin: the Late Palaeozoic Itararé Group, Paraná Basin, Brazil. Sedimentology 40, 1-25.

Feng, M., van der Lee, S., Assumpção, M., 2007. Upper mantle structure of South America from joint inversion waveforms and fundamental mode group velocities of Rayleigh waves. Journal of Geophysical Research 112, 1-16.

Fischer, K.M., 2002. Waning buoyancy in the crustal roots of old mountains. Nature 417, 933-936.

Fishwick, S., Heintz, M., Kennett, B. L. N., Reading, A. M., Yoshizawa, K., 2008. Steps in lithospheric thickness within eastern Australia, evidence from surface wave tomography. Tectonics 27, 1-17.

Frimmel, H. E., Frank, W., 1998. Neoproterozoic tectno-thermal evolution of the Gariep Belt and its basement, Namibia and South Africa. Precambrian Research 90, 1-28.

Gallagher, K., Demitru, T. A., Gleadow, A. J. W., 1994. Constraints on the vertical motion of eastern Australia during the Mesozoic. Basin Research 6, 77-94.

Garfunkel, Z., 2002. Early Paleozoic sediments of NE Africa and Arabia: Products of continental-scale erosion, sediment transport and deposition. Israeli Journal of Earth Sciences 51, 135-156.

Gee, D.G., Stephenson, R.A., 2006. The European lithosphere: an introduction. In: Gee, D.G., Stephenson, R.A., (Eds.), European Lithosphere Dynamics, Vol. 32, London, Geological Society Memoirs, p. 1-9.

Glen, R. A., 2005. The Tasmanides of Eastern Australia, In: Vaughan, A. P. M., Leat, P. T., Pankhurst, R. J., (Eds.), Terrane Process at the Margins of Gondwana, Volume 246, Geological Society, London, Special Publications, pp. 23-96.

Glen, R.A., 2013. Refining accretionary orogen models for the Tasmanides of eastern Australia. Australian Journal of Earth Sciences 60, 315-370.

Guiraud, R., Bosworth, W., 1999. Phanerozoic geodynamic evolution of northeastern Africa and the northwestern Arabian platform. Tectonophysics 315, 73-108.

Gurnis, M., 1992. Rapid continental subsidence following the initiation and evolution of subduction. Science 255, 1556-1558.

Gurnis, M., Muller, R.D., Moresi, L., 1998. Cretaceous vertical motion of Australia and the Australian-Antarctic discordance. Science 279, 1499-1504.

Hansen, S. E., Rodgers, A. J., Schwartz, S. Y., Al-Amri, A. M. S., 2007. Imaging ruptured lithosphere beneath the Red Sea and Arabian Peninsula. Earth and Planetary Science Letters 259, 256-265.

Haq, B.U., Schutter, S.R., 2008. A chronology of Paleozoic sea-level changes. Science 322, 64-68.

Heine, C., Müller, R. D., Steinberger, B., Torsvik, T. H., 2008. Subsidence in intracontinental basins due to dynamic topography. Physics of the Earth And Planetary Interiors 171, 252-264.

Holt, P., Allen, M. B., van Hunen, J., Bjørnseth, H. M., 2010. Lithospheric cooling as a basin forming mechanism within accretionary crust. Tectonophysics 495, 184-194.

Huang, J., and S. Zhong (2005), Sublithospheric small-scale convection and its implications for the residual topography at old ocean basins and the plate model, J. Geophys. Res., 110, B05404, doi:10.1029/2004JB003153

Hyndman, R.D., Currie, C.A., Mazzotti, S.P., 2005. Subduction zone backarcs, mobile belts and orogenic heat. GSA Today 15, 4-10.

Jahn, B.M., Wu, F.Y., Chen, B., 2000. Massive granitoid generation in Central Asia: Nd isotope evidence and implication for continental growth in the Phanerozoic. Episodes 23, 82-92.

Jimenez-Munt, I., Fernandez, M., Saura, E., Verges, J., Garcia-Castellanos, D., 2012. 3-D lithospheric structure and regional/residual Bouguer anomalies in the Arabia-Eurasia collision (Iran). Geophysical Journal International 190, 1311-1324.

Kaislaniemi, L., van Hunen, J., Allen, M.B., Neill, I., 2014. Small-scale convection as the mechanism for generating collision zone magmatism. Geology 42, 291-294.

Konert, G., Afifi, A.M., Al-Hajri, S.A., Droste, H.J., 2001. Paleozoic stratigraphy and hydrocarbon habitat of the Arabian plate. GeoArabia 6, 407-442.

Korsch, R. J., Harrington, H. J., Wake-Dyster, K. D., O'Brien, P. E., Finlayson, D. M., 1988. Sedimentary basins peripheral to the New England Orogen: their contribution to understanding New England tectonics, In: Kleeman, D., (Ed.), New England Orogen, Tectonics and Metallogenesis. Armidale, Australia, University of New England, pp. 134-140.

Kusky, T.M., Windley, B.F., Safonova, I., Wakita, K., Wakabayashi, J., Polat, A., Santosh, M., 2013. Recognition of ocean plate stratigraphy in accretionary orogens through Earth history: A record of 3.8 billion years of sea floor spreading, subduction, and accretion. Gondwana Research 24, 501-547.

Liégeois, J. P., Black, R., Navez, J., Latouche, L., 1994. Early and Later Pan-African orogenies in the Aïr assembly of terranes (Tuareg shield, Niger). Precambrian Research 67, 59-88.

Lüning, S., Craig, J., Fitches, B., Mayouf, J., Busrewil, A., El Dieb, M., Gammudi, A., Loydell, D., McIlroy, D., 1999, Re-evaluation of the petroleum potential of the

Kufra Basin (SE Libya, NE Chad): does the source rock barrier fall? Marine and Petroleum Geology 16, 693-718.

Matthews, K.J., Hale, A.J., Gurnis, M., Muller, R.D., DiCaprio, L., 2011. Dynamic subsidence of Eastern Australia during the Cretaceous. Gondwana Research 19, 372-383.

Mazzarini, F., Corti, G., Mazzarini, F., Corti, G., Manetti, P., Innocenti, F., 2004. Strain rate and bimodal volcanism in the continental rift: Debre Zeyt volcanic field, northern MER, Ethiopia. Journal of African Earth Sciences 39, 415-420.

McGillivray, J. G., Husseini, M. I., 1992. The Palaeozoic petroleum geology of Central Arabia. AAPG Bulletin 76, 1473-1490.

McKenzie, D., 1978. Some remarks on the development of sedimentary basins. Earth and Planetary Science Letters 40, 25-32.

McKenzie, D., Jackson, J., Priestley, K., 2005. Thermal structure of oceanic and continental lithosphere. Earth and Planetary Science Letters 233, 337-349.

Milani, E. J., De Wit, M. J., 2008. Correlations between the classic Paraná and Cape - Karoo sequences of South America and southern Africa and their basin infills flanking the Gondwanides: du Toit revisited, In: Pankhurst, R. J., Trouw, R. A. J., Brito Neves, B. B., De Wit, M. J., (Eds.), Pre-Cenozoic correlations across the South Atlantic region, vol. 294. Special Publications. Geological Society, London, 319-342.

Natal'in, B. A., Şengör, A. M. C., 2005. Late Palaeozoic to Triassic evolution of the Turan and Scythian platforms; the pre-history of the palaeo-Tethyan closure. Tectonophysics 404, 175-202.

Neves, B.B.D., Fuck, R.A., 2013. Neoproterozoic evolution of the basement of the South-American platform. Journal of South American Earth Sciences 47, 72-89.

Nikishin, A. M., Ziegler, P. A., Panov, D. I., Nazarevich, B. P., Brunet, M.-F., Stephenson, R. A., Bolotov, S. N., Korotaev, M. V., Tikhomirov, P. L., 2001. Mesozoic and Cainozoic evolution of the Scythian Platform - Black Sea - Caucasus domain, In: Ziegler, P. A., Cavazza, W., Robertson, A. H. F., Crasqui-Soleau, S., (Eds.), Peri-Tethyan rift/wrench basins and passive margins, Volume 6. Paris, Mémoires du Muséum national d'Histoire Naturelle, pp. 295-346.

Oliveira, D. C. d., Mohriak, W. U., 2003. Jaibaras trough: an important element in the early tectonic evolution of the Parnaíba interior sag basin, Northern Brazil. Marine and Petroleum Geology 20, 351-383.

Park, Y., Nyblade, A. A., Rodgers, A. J., Al-Amri, A., 2008. S wave velocity structure of the Arabian Shield upper mantle from Rayleigh wave tomography. Geochemistry Geophysics Geosystems, 9, Article Number Q07020.

Parsons, B., Sclater, J.G., 1977. An analysis of the variation of of the ocean floor bathymetry and heat flow with age. Journal of Geophysical Research, 108, 803-827.

Pasyanos, M. E., 2010. Lithospheric thickness modeled from long-period surface wave dispersion. Tectonophysics 481, 38-50.

Pasyanos, M. E., Nyblade, A. A., 2007. A top to bottom lithospheric study of Africa and Arabia. Tectonophysics 444, 27-44.

Priestley, K., McKenzie, D., 2006. The thermal structure of the lithosphere from shear wave velocities. Earth and Planetary Science Letters 244, 285-301.

Sclater, J.G., Christie, P.A.F., 1980. Continental stretching; an explanation of the post-Mid-Cretaceous subsidence of the central North Sea basin. Journal of Geophysical Research 85, 3711-3739.

Şengör, A.M.C., Natal'in, B.A., 1996. Paleotectonics of Asia: fragments of a synthesis., In: Yin, A., Harrison, M. (Eds.), The Tectonic Evolution of Asia. Cambridge University Press, Cambridge, pp. 486-640.

Stern, R. J., 1994. Arc assembly and continental collision in the Neoproterozoic East African orogen: Implications for the consolidation of Gondwanaland. Annual Review of Earth and Planetary Science 22, 319-351.

Tankard, A., Welsink, H., Aukes, P., Newton, R., Stettler, E., 2009. Tectonic evolution of the Cape and Karoo basins of South Africa. Marine and Petroleum Geology 26, 1379-1412.

Thomas, J. C., Cobbold, R., Shein S., Le Douaran, S., 1999. Sedimentary record of late Paleozoic to Recent tectonism in central Asia - analysis of subsurface data from the Turan and south Kazak domains. Tectonophysics 313, 243-263.

Turcotte, D. L., Schubert, G., 2002. Geodynamics, Cambridge, Cambridge University Press.

Turner, B. R., Armstrong, H. A., Holt, P., 2011. Visions of ice sheets in the early Ordovician greenhouse world: Evidence from the Peninsula Formation, Cape Peninsula, South Africa. Sedimentary Geology 236, 226-238.

Van Hinsbergen, D.J.J., Buiter, S.J.H., Torsvik, T.H., Gaina, C., Webb, S.J., 2011. The formation and evolution of Africa from the Archaean to Present: introduction. In: Van Hinsbergen, D.J.J., Buiter, S.J.H., Torsvik, T.H., Gaina, C., Webb, S.J., (Eds.), Vol. 357: London, Geological Society Special Publications, p. 1-8.

van Hunen, J., Zhong, S., Shapiro, N.M., Ritzwoller, M.H., 2005. New evidence for dislocation creep from 3-D geodynamic modeling of the Pacific upper mantle structure. Earth and Planetary Science Letters 238, 146-155.

van Keken, P. E., 2003. The structure and dynamics of the mantle wedge. Earth and Planetary Science Letters Frontiers 215, 323-338.

Veevers, J.J., 2006. Updated gondwana (Permian-Cretaceous) earth history of Australia. Gondwana Research 9, 231-260.

Watts, A. B., Ryan, W. B. F., 1976. Flexure of the lithosphere and continental margin basins. Tectonophysics 36, 25-44.

Williams, H., Hoffman, P.F., Lewry, J.F., Monger, J.W.H., Rivers, T., 1991. Anatomy of North America: thematic geologic portrayals of the continent. Tectonophysics 187, 117-134.

Xiao, W., Windley, B.F., Badarch, G., Sun, S., Li, J., Qin, K., Wang, Z., 2004. Palaeozoic accretionary and convergent tectonics of the southern Altaids: implications for the growth of Central Asia. Journal of the Geological Society 161, 339-342.

Zalán, P. V., Wolff, S., Astolfi, M. A. M., Vieira, I. S., Concelção, J. C. J., Appi T., Neto, E. V. S., Cerqueira, J. R., Marques, A., 1990. The Paraná Basin, Brazil, In: Leighton, M. W., Kolata, D. R., Oltz, D. F., Eidel, J. J., (Eds.), Interior Cratonic Basins. AAPG memoir 51. Tulsa Oklahoma, pp. 681-708.

Zhao, D., Hasegawa, A., Kanamori, H., 1994. Deep structure of Japan subduction zone as derived from local, regional, and teleseismic events. Journal of Geophysical Research 99, 22313-22329.

Zor, E., Sandvol, E., Gürbüz, C., Türkelli, N., Seber, D., Barazangi, M., 2003. The Crustal structure of the East Anatolian plateau (Turkey) from receiver functions. Geophysical Research Letters 30, 8044-8048.

Figure captions

Fig. 1. Age of assembly of continental crust. This is not necessarily the age of the units within each area, but the age at which that region of crust was assembled as a unit. This is a compilation of data from numerous publications covering South America (Almeida et al., 2000; Milani and De Wit, 2008), North America (Canil, 2008; Williams et al., 1991), Europe (Gee and Stephenson, 2006), Africa and Arabia (Begg et al., 2009; Van Hinsbergen et al., 2011), Asia (Şengör and Natal'in, 1996) and Australia (Debayle and Kennett, 2003).

Fig. 2. Locations of basins, wells and pseudo-wells in this study; (a) Location map of the Palaeozoic intracratonic basins in South America. Wells from the Paraná Basin from Milani and De Wit (2008) and Zalán et al (1990); (b) The extent of the Cape-Karoo Basin of South Africa (Tankard et al., 2009). The location of the outcrop sections used to make up the subsidence curve for the Cape Fold Belt is shown by the circle. The composite sections used by Cloetingh et al (1992) are used for pseudo-wells Cape 1 and Cape-Karoo 2, representative of west of 20^{o} E (Western Cape) and east of 24^{o} E (Southeastern Cape); (c) The extent of sediments beneath the Hercynian unconformity (roughly Late Carboniferous in age) across Arabia. The location of the Khanaser #1 well in Syria and the outcrop study used for the backstripping are both located upon the map; (d) A map of the sedimentary cover over the Turan and Scythian platforms take from (Natal'in and Şengör, 2005; Thomas et al., 1999). In the absence of usable well data a cross-section (Thomas et al., 1999) has been used as input for the backstripping. The location of the cross-section is shown on the map. The four 'pseudo wells' from the cross-section are marked; (e) The Mesozoic-Cenozoic cover of Eastern Australia. The extent of the sedimentation is taken from Gallagher et al. (1994). The location of the depocentres mentioned in the text and the wells used in the backstripping are shown on the map. The abbreviations for each of the wells are as follows. W = Walkandi 1, C = Cook North 1, L = Lowood 1, R = Red Cap 1 and A = Arlington 1.

Fig. 3. The backstripped subsidence curves for the Paraná Basin and the PreCordillera compared with the best fitting forward models. The sources of the three curves from the Paraná Basin are explained in the text, and wells for the Paraná Basin are located on Fig. 2a. Well A is from the PreCordillera, B and C are from the main Paraná Basin, using data in Milani and DeWit (2008) and versions of the stratigraphy from both Zalán et al (1990) and Eyles et al (1993). The best fitting model for the Paraná Basin has a 36 km crust and a final lithosphere thickness of 130 km. The PreCordillera is best fitted by a model with a 30 km thick crust, but the same final lithosphere thickness.

Fig. 4. Backstripped subsidence curves from the outcrop data in the Cape Fold Belt (A) and from two pseudo wells in the wider Cape-Karoo Basin (B and C). See Fig. 2b for location information. The best fit forward models to each of these subsidence curves are shown alongside the backstripping. All the best fit models have a final lithospheric thickness of 122 km. The Cape Fold Belt is fitted by a 23 km thick crust and the wider Cape-Karoo Basin by a 27 km thick crust.

Fig. 5. The Palaeozoic sediments of Arabia contain a number of eroded sections which shows in the backstripped subsidence curves as flat areas with no subsidence. The best fitting subsidence curves from the forward model are shown alongside the backstripping. The Khanaser #1 well (A) is fitted best by a 30 km thick crust and 122 km thick final lithosphere. The outcrop data are fitted best by a 33 km thick crust and a 139 km lithosphere (B). Locations of the well and outcrop data are shown on Fig. 2c.

Fig. 6. The results of the backstripping from the four pseudo-wells in the Turan platform (located on Fig. 2d). The best fitting models for each well all have a final lithospheric thickness of 155 km. The best fitting crustal thickness for the Khiva Depression (A) is 28 km, 30 km is used for both Amu Dar'ya 1 and 2 (B and C) and a 31 km thick crust is used for Chardhzu (D).

Fig. 7. The backstripped subsidence curves from the platformal succession of Eastern Australia compared to the curves produced by the best fitting forward model. The locations of the wells are shown on Fig. 2e. The best fitting model varies from Walkandi 1 well in the west which is fitted best by a model with a 154 km thick lithosphere and a 38 km thick crust (A). The best fitting crust gets thinner as does the lithosphere to the east, through the Cook North 1 (B), Lowood 1 (C) and Red Cap 1 (D) wells, with the Arlington 1 well (E) being fitted best by a 32 km thick crust and a 122 km thick final lithosphere.

*Revised manuscript with no changes marked
Click here to view linked References

Basin formation by thermal subsidence of accretionary orogens

P.J. Holt, M.B. Allen* and J. van Hunen

Department of Earth Sciences, University of Durham, Durham, DH1 3LE, UK

***tel: +44 (0)191 3342344; fax: +44 (0)191 3342301; e-mail: m.b.allen@durham.ac.uk**

Abstract

Subsidence patterns of 18 stratigraphic sections from five sedimentary basins around the world are analysed by forward and inverse modelling, in order to explain the mechanisms by which basins form on the juvenile crust generated by accretionary orogens. Study areas are the Paraná Basin (Brazil), Karoo Basin and Cape Fold Belt (South Africa), the Arabian Platform, Scythian and Turan platforms (Central Asia) and eastern Australia. The form of the tectonic subsidence curves derived from backstripping analysis is consistent with results from a forward model, which produces thermal subsidence of crust with normal thickness (~35 km) but low initial mantle lithosphere thickness. This high thickness ratio of crust:mantle lithosphere is the plausible initial configuration of lithosphere produced by accretionary tectonics. Our results do not require late stage orogenic extension or lithosphere delamination as a precursor to the thermal subsidence phase.

Keywords: basin; accretionary crust; thermal subsidence; juvenile

1. Introduction

The subsidence mechanism of intercratonic (intracontinental, or simply cratonic) basins has long been debated. These broad, uniform, basins are not easily explained by either rifting or lithospheric flexure (Allen and Allen, 2005). Holt et al (2010) studied the Ghadames and Kufra basins, North Africa, and suggested that their Palaeozoic subsidence was a consequence of the formational properties of the region's Neoproterozoic accretionary crust (Bumby and Guiraud, 2005; Caby and Monié, 2003; Guiraud and Bosworth, 1999). Such crust inherits the thin mantle lithosphere of many of its constituent building blocks (island arcs, accretionary wedges and young oceanic crust), and as this cools and thickens following tectonic assembly it causes subsidence as an isostatic response. However, it has not yet been proven if the process is an inherent property of juvenile crust generated by accretionary orogeny (Cawood et al., 2009), and therefore generally applicable. This paper aims to test this subsidence mechanism by looking at an overview of the subsidence patterns from a number of regions of accretionary crust.

Accretionary crust is defined as continental crust which forms during an accretionary orogen, which unlike a collisional orogen overlies at least one active oceanic subduction zone throughout its history (e.g. Şengör and Natal'in, 1996; Xiao et al., 2004; Collins et al., 2011; Kusky et al., 2013). It may also be referred to as juvenile crust (in relation to older cratonic crust). Accretionary orogens occur on the margins of a pre-existing continental nuclei, and are a focus for crustal growth. For example, the majority of granitoids from the Central Asian Orogenic Belt consist of high proportions (60 to 100%) of mantle-derived material (Jahn, 2000). Accretionary crust can vary in thickness from <30 km to >50 km. It is made up of differing terranes including island arcs, slivers of back arc crust, accretionary wedges from the forearc, slices of obducted oceanic crust and older microcontinental blocks embedded in broad collages of more juvenile material.

A key aspect of such crust is that it may be of near normal thickness, but is commonly underlain by thin mantle lithosphere at the time of accretion (e.g. Zhao et al., 1994; Zor et al., 2003). The reason for this is that the tectonic and magmatic processes that produce such crust are not necessarily complemented by equivalent processes to form an underlying mantle lithosphere. For example, slivers of a subducting plate may be scraped-off and accumulate to form an accretionary wedge above the subduction zone, but this is a process that builds crust, not mantle lithosphere. Also, before final accretion and the end of subduction, corner flow of the hydrated, weak mantle wedge may act to limit and reduce mantle lithosphere thickness (e.g. Eberle et al., 2002; Hyndman et al., 2005). Once final subduction has ceased under an accretionary orogeny, any such thin mantle lithosphere will tend to thicken, in the manner of lithosphere thinned after a rifting event (McKenzie, 1978), with the crucial difference that there need not have been any such stretching event to produce the thin mantle lithosphere.

Ultimately, such accretionary orogens may be the principal sites for net crustal growth, and have operated as such back into the Archaean (Cawood et al., 2009). The ages of accretion for the continental crust are shown in Fig. 1. Dimensions may be vast: 1000s x 1000s of km.

Many of these accretionary orogens have large, intact, platformal sedimentary sequences that accumulated upon them. This study examines the Paraná Basin, Cape Fold Belt and Karoo Basin, Arabian Platform, Scythian and Turan platforms and the post-Tasmanide basins of eastern Australia. These areas represent basins established over accretionary crust that formed at various times ranging from the Neoproterozoic to the Mesozoic. The global spread of the study areas gives confidence that we are dealing with a fundamental process, rather than a localised phenomenon. Basins were chosen because they are large, representative features for which data are available; there was no filtering of locations to try and find the best fits to the proposed model.

A number of other subsidence mechanisms have been suggested for these basins. Recently, it was suggested that many such basins form due to stretching of the continental lithosphere at low strain rates for long periods of time (50 – 100 Myrs) (Armitage and Allen, 2010). This produces a subsidence profile that begins with a straight line during the stretching phase, and then has a slight kink followed by a curved section caused by cooling acting over the stretched area. Dynamic topography has been suggested as an appropriate basin-forming mechanism (e.g. Gurnis, 1992), whereby subsidence is related to large-scale mantle flow patterns. It has also been suggested that regional subsidence is due to orogenic collapse following an accretionary orogeny, because the mantle lithosphere undergoes delamination (Ashwal and Burke, 1989, Burke et al., 2003). This scenario envisions a high density of small rifts, similar to the Basin and Range province, followed by a period of broad scale uniform subsidence with an exponential decay as the delaminated lithosphere is replaced by cooling upper mantle. Avigad and Gvirtzman (2009) suggested that there was partial mantle lithosphere detachment under the Arabian region in the Late Proterozoic, leading to initial surface uplift, but subsequent cooling and subsidence. There are similarities between this model and our study (in that both models envisage thermal subsidence as thin lithosphere cools and thickens), but we do not require the initial detachment.

There are many other mechanisms which have been suggested for individual basins, such as simple rifting (Oliveira and Mohriak, 2003) or back arc extension (Thomas et al., 1999), and flexure to create a foreland basin (Catuneanu, 2004; Milani and De Wit, 2008). We propose that the large scale and geometry of each of the basins in this study are incompatible with these “conventional” mechanisms. For example, the Palaeozoic basins of North Africa and Arabia represent an original “megabasin” covering ~10,000,000 km^2 from the Atlantic margin to the eastern edge of Arabia. Allowing for continental fragments now dispersed within Iran and adjacent countries, it was probably once even larger (Şengör and Natal’in, 2006).

2. Methodology

The first step in assessing the cause of the subsidence in each region is to backstrip the sedimentary record to get the tectonic subsidence of the region, i.e. inverse modelling. Results can then be compared to subsidence produced by a numerical forward model of thickening and cooling of the mantle lithosphere.

Backstripping is the process of calculating the tectonic subsidence from a sedimentary column. The practice is commonplace and the approach used here follows that of Watts and Ryan (1976), described in detail in Holt et al. (2010). We use standard relationships from published work (Sclater and Christie, 1980) for the porosity-depth relationships. A global eustatic sea-level curve (Haq and Schutter, 2008) is used to remove the effects of sea-level changes. Some of the study areas already have backstripped subsidence curves available in the literature. In other areas backstripping was carried out using available published records of the stratigraphy, either from well data, regional cross-sections constructed using seismic data, or regional stratigraphic columns based on thicknesses from fieldwork studies. In each region different data sources are used if available, to allow comparison between subsidence curves calculated from different data sets. Where there is disagreement in the literature as to the ages of the sediments, a subsidence curve is calculated for each conflicting interpretation.

The subsidence produced by thickening and cooling of the lithosphere beneath accretionary crust is calculated using a numerical forward model described in Holt et al. (2010), and explained below. This model calculates the conductive heat flow through a column of crust and upper mantle material and then the resultant subsidence of the column. The subsidence calculated is water loaded tectonic subsidence and therefore is directly comparable to that calculated from the backstripping.

The numerical subsidence model is based on and tested against the plate models for sea floor spreading (Parsons and Sclater, 1977). It is modified to include layered continental crust with radioactive heat production. It solves the vertical conductive heat flow through a one-dimensional column of the lithosphere and upper mantle:

$$\rho C_p \frac{\partial T}{\partial t} = \frac{\partial}{\partial z}(k \frac{\partial T}{\partial z}) + A \quad (1)$$

Equation 1 is solved using a finite difference technique with a grid resolution of 1 km. *T* is the temperature of the rock at a particular point in the grid at depth *z*. *A* is the contribution of radioactive heat production and *t* is the time over which the temperature is changing. Time-stepping is performed with an forward Euler time-integration scheme. The material properties of the rock are the thermal conductivity (*k)*, the specific heat capacity (C_p) and the density (ρ). The density of the rock is dependant on the temperature and is calculated using equation 2.

$$\rho = \rho_0(1 - \alpha(T - T_0)) \quad (2)$$

In Equation 2 the reference density (ρ_0) and the coefficient of thermal expansion (α) are dependent on the rock type. The values used for all the parameters in Equations 1 and 2 follow Holt et al. (2010).

The model has a felsic upper crust and granulitic lower crust, which is underlain by mantle lithosphere. The base of the lithosphere is purely thermal rather than compositional and is defined by the temperature below which the mantle rock does not deform significantly over geological timescales. The 1200 °C isotherm is used (Turcotte and Schubert, 2002). The model starts with a 20 km thick mantle lithosphere, to represent the initial thin mantle lithosphere typical of accretionary orogens at the time of their formation. The temperature at the surface of the model is set as 0°C. The temperature at the base of the model is calculated using the potential temperature (i.e. a given mantle temperature extrapolated to the surface) and an adiabatic gradient of 0.3°C per km. Constant temperature boundary conditions are used at the top and bottom of the model. The initial temperature conditions follow this mantle adiabat to

up to a transition point 20 km below the crust above which they follow a linear gradient to the surface. The depth and therefore temperature at this transition point is dependent on the thickness of the crust and the potential temperature for the surface. The elevation is calibrated from the density profile of the column using a column of hot mid ocean ridge material with a 7 km thick basaltic-gabbroic crust at 3 km below sea-level as reference. Standard Pratt isostasy is used. When the topography of the model drops below sea level the basin is filled with water. The thermal boundary condition is applied to the basement floor because water in the basin would have an almost uniform temperature due to convection. However, the water is included in the isostacy so the model effectively produces water loaded tectonic subsidence.

One inherent weakness of the plate model is that it only calculates the heat transfer by conduction (Parsons and Sclater, 1977). At the base of the plate heat transfer changes from conduction to convection (e.g. van Hunen et al., 2005). The plate model does not explicitly describe the physics of this transition, but provides a good fit to the bathymetry and heatflow data (Huang and Zhong, 2005). Gravitational instabilities of the thickening lithosphere are not explicitly included in our model, but the average reduction in lithospheric thickening of any detaching or delaminating lithosphere is accounted for by the plate model.

We ignore the temperature dependence of k, C_p and α. This assumption slightly overestimates temperatures in the top half of the model and underestimates temperatures in the bottom half of the model (McKenzie et al., 2005). This means the depth to the base of the lithosphere is an upper limit. We do not model metamorphic reactions in the cooling lithosphere (Fischer, 2002).

The modelled subsidence is most sensitive to variations in the thickness of the crust and the final thickness of the lithosphere, which is controlled by the model thickness (plate thickness) (Holt et al., 2010). Therefore these two parameters are varied to find the column of lithosphere and crust which best fits the observed subsidence for each region, as represented

by the backstripped subsidence curves. Other parameters are kept constant between the different models. The best crust and lithosphere thickness values produced by the forward modelling are compared to published measurements of the crustal and lithospheric thickness, to see if model values are realistic. There is a caveat here that we have to use present day thickness values, leaving it possible that these have changed since the end of basin formation, which was 100s of millions of years ago in some of the examples we study. To minimise this effect we have used basins and sections from regions that have not been heavily overprinted by later tectonic events, although departures from idealised behaviour are present in some of the curves, and are discussed individually in the Results section.

3. Regional geology

Each region is looked at in turn in this section, considering both the accretion history of the area and the basins formed on the juvenile crust. It is not the intention to review each region in exhaustive detail, rather the aim is to give an overview, and compare the subsidence across different regions in section 4.

3.1 South America: Paraná Basin

Much of western Brazil and Argentina are made up of crust accreted in the Brasiliano orogeny (Bumby and Guiraud, 2005). Before the formation of the Atlantic, this was a continuous band of accretionary crust that formed in the Late Proterozoic (Neves and Fuck, 2013). The assembly of the North African accretionary crust appears to have finished marginally earlier with the final phase of accretion occurring at ~600 Ma, dated using orogenic granites (Liégeois et al., 1994). Similar batholiths in the Brasiliano collage formed between 590 and 500 Ma (Almeida et al., 2000). The crust is not exclusively made up of juvenile terranes, but includes numerous older Proterozoic and even some Archaean blocks (Brito Neves, 2002).

However, these are reworked during the orogeny and should not affect the initial conditions of a thin lithosphere suggested in the subsidence mechanism being tested.

There are a number of basins situated in this region, such as the Parnaíba Basin, the Paraná Basin and its extension into Argentina, the Choco-Paraná Basin, shown in Fig. 2a. The Paraná Basin is situated in southern Brazil and covers an area of over 2 million km^2 (Fig. 2a). The earliest sediments within it date from the late Ordovician, and the sedimentary succession continues through to the Jurassic where it is capped by lavas of the Serra Geral, which are related to rifting of the Atlantic margin. Detailed descriptions of the sedimentary fill are given in Zalán et al., (1990) and Eyles et al., (1993). The earliest strata are known as the Silurian sequence, although it starts with continental sandstones and conglomerates of Middle to Late Ordovician age (Zalán et al. (1990) and Eyles et al. (1993) disagree as to exactly when deposition started).

These rocks change gradationally into shales and siltstones of Silurian age, and to shallow marine sandstones by the end of the Silurian. There was a period of erosion during the Early Devonian, followed by deposition of the Devonian sequence. Again, this shows a complete transgressive – regressive cycle, beginning with transgressive sandstones, fining up into marine shales, which are overlain by deltaic sandstones. This deposition was followed by another hiatus and further erosion, which lasted for much of the Carboniferous. Sedimentation began again with continental redbeds at ~ 270 Ma, followed by deposition of glacial marine sediments and another transgressive – regressive cycle during the Permian. There is some disagreement between different authors. Eyles et al., (1993) showed continuous sedimentation through to the base of the Serra Geral lavas, whereas Zalán et al., (1990) reported a hiatus during the Lopingian (end Permian) and Early Triassic. Both sets of authors agree the overlying Triassic sediments are entirely continental, consisting of lacustrine, fluvial

and aeolian sediments that continue into the Jurassic. Jurassic strata are interbedded with the Serra Geral lavas.

3.2 Southern Africa: Cape Fold Belt and the Karoo Basin

The Cape Fold Belt and the Karoo Basin in southern Africa (Fig. 2b) have similar sedimentary fills to the Paraná Basin described above. The subsidence patterns are also similar, leading to a number of correlations being suggested (Milani and De Wit, 2008). However, unlike South America the African regions are not entirely underlain by accretionary crust (Fig. 1). The Cape Fold Belt is largely underlain by Neoproterozoic accretionary crust of the Damara Belt, which forms part of the same mobile belt as the South American accretionary crust. The Cape-Karoo Basin to the north is underlain by Mesoproterozoic basement, and its western side is floored by Archaean basement of the Kaapvaal craton (Milani and De Wit, 2008). If the subsidence mechanism suggested also formed the Cape-Karoo Basin then the older crust must have been remobilised by the Pan African orogeny. This is supported by evidence from the Mesoproterozoic basement flanking the Damara belt which has been rejuvenated (Frimmel and Frank, 1998). Also the basement of the combined Cape-Karoo Basin is intruded by Cambrian A-type granites indicating involvement in the accretion process (Milani and De Wit, 2008). A similar situation is seen in the North African accretionary crust, where there is evidence for reworking of a Palaeoproterozoic cratonic block during the Pan African, and the existence of the older crust has no discernible effect on the subsidence patterns (Abdelsalam et al., 2002).

This pattern suggests that the crustal accretion processes of juvenile orogens can lead to tectonic reactivation and thinning of neighbouring lithosphere. This effect could be because during the accretion there is an intervening ocean subducting beneath the older crust, and the

subduction process leads to thinning the older lithosphere through corner flow or back arc stretching (Arcay et al., 2006; van Keken, 2003). Sedimentation in both the Cape Fold Belt and the Cape-Karoo Basin began with a succession of mature, continental-derived, siliciclastic sediments. Deposition began sometime in the mid Cambrian, although this timing is difficult to date, and continued until the Devonian. Strata show glacial influence during the Ordovician, followed by shales that represent maximum flooding of the Ordovician to Silurian transgressive – regressive cycle (Turner et al., 2011). Unlike the Paraná Basin, there is no significant hiatus before the Devonian cycle. The sedimentation is similar in character to the Paraná, showing a transgressive – regressive cycle with silt and mudstones representing the maximum flooding, which shallow upwards to Early Carboniferous lacustrine sediments. These Carboniferous strata are the youngest preserved sedimentary rocks in the Cape Fold Belt (Turner et al., 2011).

In the Cape-Karoo Basin the Carboniferous lacustrine rocks are overlain by glaciogenic sediments made up of diamictites and rhythmites, which continued until the Early Permian. These strata are succeeded by black mudstones, grading into deltaic sands. There is some debate as to whether the glaciogenic sediments and those following are deposited into a marine or lacustrine environment (Milani and De Wit, 2008). At the end Permian there is a deepening of the basin as black shale is deposited. There is then a gradual shallowing evidenced by distal turbidites passing upwards into coarser turbidites and ultimately shoreline and fluvial deposits. From this point on the sediments are terrestrial, represented by desertification throughout the Triassic. The sequence is terminated by the eruption of the Karoo Large Igneous Province in the Jurassic. A more detailed overview of the sedimentary history of the Cape Fold Belt can be found in Turner et al., (2011) and for the Cape-Karoo Basin in Milani and De Wit, (2008).

3.3 Arabia

The Arabian crust also forms part of the accretionary crust formed during the Pan African orogeny, and was contiguous with counterparts in North Africa before the opening of the Red Sea. Proterozoic basement is particularly well exposed along the flanks of the Red Sea due to Cenozoic surface uplift at the margins of that rift zone. Therefore the region provides good insight into the makeup and assembly process of accretionary crust. The Arabian crust is composed of numerous sutured terranes. Many of these terranes are island arcs, dated between 870 – 690 Ma (Stern, 1994). There are also ophiolitic terranes, accretionary wedges (not to be confused with accretionary crust) and older terranes from the Meso-Palaeoproterozoic. In his area of study Stern, (1994) described roughly two thirds of the crust as juvenile. The geochemistry of xenoliths brought up from the lower crust and mantle by Miocene and younger volcanics in Syria, Jordan and Saudi Arabia confirms that regions with sedimentary cover are also underlain by juvenile basement, made up of Neoproterozoic island arc terranes (Al-Mishwat and Nasir, 2004). The accretion was a gradual process with some terranes colliding with each other to form composite terranes, before colliding in the main accretionary orogen. The date of the final phase of accretion is ~550 Ma in the east of Arabia, but gets progressively younger westwards, and is ~500 Ma on the flank of the Red Sea (Stern, 1994).

Apart from where the basement is exposed alongside the Red Sea most of Arabia is blanketed by Palaeozoic sediments (Konert et al., 2001), as shown in Fig. 2c, which collectively form the Arabian Platform. The earliest sediments are continental clastics which are Cambrian in age. These were deposited in the north and east, but are not seen in the southwest of Arabia. During the Ordovician the marine influence spread inland, and the area of deposition expanded to the southwest. Even so, Early Ordovician sediments are mostly sandstones except along the fringes of the platform. These were overlain by fine grained clastics in the Mid Ordovician. The Late Ordovician saw a period of glaciation with widespread erosion inland and glaciogenic deposition near the edges of the platform. This was followed by filling of the glacial

topography with coarse clastics and then a widespread transgression during the Silurian. In the Early Silurian shales were deposited, which are an important source rock for hydrocarbons in some areas. The sediments then record the transgressive phase of the cycle coarsening upwards into shoreface and deltaic sandstones. More detail is available in Garfunkel (2002), who notes that the same sedimentary patterns are seen across much of North Africa and therefore concludes that it formed a 2000 km wide platform. As Fig. 2c shows, later sediments are not as well preserved and have a patchier distribution.

There was then a hiatus in sedimentation, which resumed in the Middle Silurian in central Arabia (McGillivray and Husseini, 1992), but did not begin until the Late Silurian further north in Syria (Best et al., 1993) or Iraq (Al-Juboury and Al-Hadidy, 2009). This hiatus was related to the "Caledonian orogeny", which is seen across North Africa as well. The quotation marks are advisable: this deformation is Early Palaeozoic in age, and for this reason commonly termed "Caledonian", but there is no simple correlation with the orogeny of that name in northwest Europe and conjugate parts of North America.

Sedimentation renewed in the Devonian in central Arabia, with a transgressive to regressive cycle that began with fluvial sediments. These rocks pass into marine sandstones with minor carbonates in the Emsian, then back into shoreface sandstones. In the north of the platform the hiatus lasted until the end of the Mid Devonian. The sequence deposited afterwards is mainly siltstones and shales, with some sandstones and minor carbonates, and the youngest rocks are from the end of the Mississippian. In both areas the top of the sediments is marked by an erosional surface referred to as the Hercynian event – with a similar caveat about the use of this term to "Caledonian". This has cut down to the Silurian sediments in some areas, so extensive section may be missing. Both areas experience subsequent phases of subsidence. However the modelling results suggest that the effect of cooling and thickening of lithosphere should be negligible by this point (> 200 Myrs after accretion has finished).

Therefore subsequent episodes of subsidence are likely to be caused by other mechanisms. This illustrates the polyphase nature of many of these basins. In Arabia, the later phases are much better studied because they host the majority of the discovered hydrocarbons (Guiraud and Bosworth, 1999).

3.4 Scythia and Turan

The platforms of Scythia and Turan (Fig. 2d) formed upon a band of accretionary crust which developed on the northern side of the Palaeo-Tethys Ocean (Fig. 1). The region is unique in this study, in that it did not lie on the margin of Gondwana. The Middle Caspian Basin lies between the Scythian and Turan platforms. The evolution of both the basement and cover of the Middle Caspian Basin probably resembles that of the adjacent areas, but as there are fewer details known it is not analysed here.

Assembly of the Scythian and Turan basement was largely a late Palaeozoic process (Şengör and Natal'in, 1996). The regional basement is penetrated by wells (Fig. 2d) that encountered a mixture of granitoids, mafic, felsic and intermediate volcanics of Carboniferous to Triassic age. Available geochemical data show a subduction-related origin for these rocks. The terranes which make up the basement are interpreted as originating mostly as paired forearc and arc units (Natal'in and Şengör, 2005). Amalgamation finished during the mid-Triassic in Turan.

Initial platform sediments overlap in age with the final phase of accretion. Sedimentation began on the Turan Platform in the Permian with continental sediments. The platform was then submerged, and sedimentation switched to marine clastics which continued into the Triassic. Thomas et al. (1999) note the main extension phase is Late Permian – Early

Triassic, interpreted to be caused by back-arc stretching. During the Late Triassic there was a period of compression, with some erosion in the north.

The earliest sedimentation on the Scythian Platform is Early Triassic in age. There are a number of north-south trending rifts (Nikishin et al., 2001). During the Late Triassic – Early Jurassic there was compression, as the Alborz terrane collided to the south during the closure of Palaeo-Tethys. This led to erosion, which obscures the original extent of the Triassic strata. The Scythian Platform remained above sea-level during the Early Jurassic. In the Middle Jurassic the east of the platform was flooded and a clastic sequence was deposited. The western side of the platform remained above sea-level. On the Turan Platform, the Early Jurassic sediments to the north and east were fluvial and deltaic, whereas in the southwest shallow marine sandstones fined upwards into silts and shales. These patterns were repeated in the Late Jurassic where a regression caused evaporites to be deposited to the north and east, while in the southwest carbonates were deposited. There was major transgression across the whole platform during the Cretaceous (Thomas et al., 1999), and marine sediments were deposited, including chalk.

There was gentle folding during the Early Paleocene before sedimentation resumed across the combined platform. Shallow marine sediments were deposited during the rest of the Paleocene and the Eocene. Sedimentation terminated across much of the Scythian Platform during the Eocene. In Turan there was a pulse of Oligocene to Quaternary subsidence caused by the collision between Arabia and Eurasia. The sediments deposited at this time are clastics shed from the rising mountains to the south.

3.5 Eastern Australia

The Tasmanides of eastern Australia were accreted from the Mid Cambrian to the Permian (Fig. 2e), a similar time scale to the accretionary crust in Arabia and North Africa.

There is a mix of terrane types including older Proterozoic crustal fragments, island arcs, accretionary complexes and ophiolitic terranes: a thorough review is provided by Glen (2005) and Veevers (2006), from which this summary is taken. Accretionary crust formed over five distinct orogens, which are marked by a period of collision of new terranes onto the margin. The collisional phase was followed by a period of extension while subduction continued along the margin of the region. This process indicates that the lithosphere remained thin until the accretion terminated, because it was being stretched after each collision phase. The earlier orogens were originally thought to contain a greater proportion of older crust, but this has been recently revised based on dating of basement from new wells (Glen, 2005; 2013). Many Proterozoic microcontinents were rejuvenated during accretion and were intruded by granitoids.

Much of the Tasmanides (10^6 km^2) are covered by platformal Mesozoic to Cenozoic sedimentary cover (Fig. 2e). The evolution of the platform is described in Gallagher et al. (1994). The earliest platform sediments are Early Permian in age. They are found in the Eromanga and Cooper basins in the west of the Tasmanides, and the Bowen-Surat-Sydney Basin, which trends north-south in the east of the region. These sediments are shallow marine clastics in the east and continental clastics (fluvial and lacustrine sediments) in the west. In the Mid Permian sedimentation ceased and there was a brief period of erosion across the platform before continental clastics were deposited during the Triassic. During the Late Triassic there was another period of erosion, which was more severe towards the east. In the Jurassic a fining-upwards succession passing from coarse sandstones to shales was deposited across the entire platform and is interpreted to be a fluvial environment, changing upwards into a lacustrine environment. The sediments contain progressively more volcanically derived material in the east suggesting there was a volcanic margin to the east of the platform. In the Early Cretaceous the basins were connected to the sea and sediments fluctuate between shallow marine and deltaic sediments in both the Eromanga and Surat basins. There was a

regression in the east around 110 Ma , and during the Cenomanian continental sediments were deposited. In the west there is a brief period of increased subsidence at 100 Ma. Sedimentation ceased shortly afterwards.

4. Results

4.1. South America

Backstripped curves for the Paraná Basin and PreCordillera were published by Milani and De Wit (2008). Published stratigraphy was also used to generate the backstripped curves in Fig. 3 alongside the best-fitting forward model curve. A pseudo-well from a cross-section through the Paraná Basin (Zalán et al., 1990) was backstripped as well, with both of the conflicting age estimates for the sediments (Eyles et al., 1993; Zalán et al., 1990).

When the backstripped curves are compared to the forward model, the first 150 Myrs shows subsidence similar to a modelled curve produced with a 36 km thick crust and a final lithospheric thickness of 130 km. Note that in Fig. 3 and subsequent similar figures, the initial part of the forward modelling curve, where the elevation was above sea level, is not shown. This represents a time of up to several 10s of millions of years and 100s of metres of subsidence that are not regionally recorded in the sedimentary record.

The fit between the backstripped and forward modelled curves is not perfect, in part because there are periods of uplift and erosion, which are evident in the backstripping, but not the forward modelling. After 310 Ma there is sudden increase in the subsidence rates. This coincides with collision of the Gondwanides along the western margin of South America. It has been suggested the Paraná Basin became a foreland basin at this time, causing renewed

subsidence (Milani and De Wit, 2008). The subsidence in the PreCordillera began ~100 Ma earlier and may reflect earlier accretion and cratonisation of the crust beneath this basin before it docked with the rest of South America. This collision at the end of the Ordovician could explain the increased subsidence observed after 400 Ma (Milani and De Wit, 2008). It is fitted best by a model with a 30 km thick crust and a 130 km thick lithosphere. The fit to the model is very close for the first 150 Ma. The results show that lithospheric cooling of accretionary crust can explain the overall subsidence seen in the basins in this region of South America, before a later phase of subsidence due to flexure in a foreland basin setting. The crustal thickness used for both basins is consistent with the results of Feng et al., (2007) who measure the Moho varying between 35 and 40 km depth beneath Paraná, and between 25 and 35 km depth beneath the PreCordillera. Lithosphere thickness is not well constrained.

4.2 South Africa

The subsidence curves for the Cape-Karoo Basin are from data in Cloetingh et al., (1992) and the curve for the Cape Fold Belt is from outcrop data in Turner et al., (2011). All these data are composite thicknesses from regional stratigraphy. Both subsidence curves for the Cape-Karoo Basin are fitted well by a forward model with an initial crustal thickness of 27 km and a final lithospheric thickness of 122 km (Fig. 4). The subsidence of the Cape Fold Belt is matched most closely by an initial 23 km thick crust and a final 122 km thick lithosphere. However, to achieve this match an unusually thin initial lithosphere of only 27 km thickness is required. If a thicker initial lithosphere was used the shape of the curve would remain the same, but the first part of it would be missing as the crust would start below sea-level.

The crustal thickness values are in agreement with present crustal thickness, which thins towards the south from ~30 km to 25 km (Pasyanos and Nyblade, 2007). The regional best fitting lithospheric thickness is also in good agreement with the lithospheric thickness measured using shear wave tomography, which is ~120 km (Priestley and McKenzie, 2006).

Therefore the model provides a good fit to the subsidence curves in South Africa using parameters which match those published in the literature, notwishstanding that this is an area that may have been affected by both compressional deformation and magmatism/extension related to the opening of the South Atlantic. Similar to South America there is a phase of renewed subsidence, which has again been attributed to growth of the Gondwanides (Milani and De Wit, 2008).

4.3 Arabia

McGillivray and Husseini, (1992) published a number of wells through the Palaeozoic section in Syria. Of these, two penetrate crystalline basement and one finishes in the Cambrian, however all three are missing sections from the Devonian and Early Mississippian. The most complete in terms of sedimentary units is the Khanaser #1 well, which is therefore used in this study (Fig. 5). Published well data from central Arabia are sparser, therefore thicknesses from outcrop have been used instead (Best et al., 1993). Fig. 5 shows the fit of the modelled subsidence to the backstripping. The outcrop data from central Arabia is fitted best by a 33 km thick crust with a 139 km final lithospheric thickness. The model parameters used to acquire the best fit for the Khanaser #1 well are a 30 km thick crust with 122 km thick lithosphere. When the sedimentary cover is added the crustal thicknesses are both broadly in agreement with the 38 km inferred by Al-Mishwat and Nasir (2004). The slightly thinner crust in the north would also provide a neat explanation for the earlier onset of sedimentation than in the south of the platform. It is not clear why there should be a difference in the best-fit final lithosphere thickness between these two regions, although it matches the thinning in a northwards direction noted by Hansen et al. (2007). Comparison to the present day lithospheric thickness is not viable because it has been affected by later events, such as the collision between Arabia and Asia in the north (Priestley and McKenzie, 2006) and the rifting of the Red Sea in the South West (Pasyanos, 2010). Published estimates for the lithosphere

thickness under Arabia vary markedly between different authors (Hansen et al., 2007; Park et al., 2008; Jimenez-Munt et al., 2012), making it difficult to compare our model results with observations.

For both the outcrop and the well the proposed subsidence mechanism provides a reasonable fit to the backstripping, but there is a lot more variance from the predicted subsidence curves taken from the modelling than in the other regions studied. This may be because of the greater amount of erosion experienced by these sections than other regions in this study. However, there is still a good temporal link between the accretion and the subsidence as well as a broad fit to the subsidence curves, despite the problems with erosion.

4.4 Scythia and Turan

Sedimentary thicknesses for the Turan platform are taken from Thomas et al. (1999). They created an isopach map of each layer using regional seismic data constrained by 500 wells. These were used by Thomas et al. (1999) to create a number of cross-sections across the platform, one of which was used to provide the inputs for the backstripping in this study. Four columns were backstripped from the cross-section to look at the difference across the platform (Fig. 6).

The fit between the forward model and backstripping are shown in Fig. 6. The deepest sequence in the Khiva depression is fitted very well by a 28 km thick crust and a 155 km thick final lithosphere. For the other three columns the fit is good except for the first point. As mentioned previously the first layer of sediment is not divided beyond Permian and Triassic, which has been followed in the backstripping. Therefore the timing for the start of subsidence has the greatest uncertainty. Equally the area was still being influenced by accretion and rifting until the mid-Triassic, which could also affect the poor fit to the start point. The other points fit well with lithospheric cooling with the reduced subsidence being explained by a slight increase

in the crustal thickness to 31 km in the east. This fits with the observations of Natal'in and Şengör, (2005) who note that the forearc terranes, which are floored by oceanic crust coincide with the deepest sedimentary cover. The lithosphere thickness was kept constant across the Turan platform and is within the range of variation suggested for the region (120-180 km) (Pasyanos, 2010; Priestley and McKenzie, 2006).

4.5 Eastern Australia

Mesozoic subsidence patterns in eastern Australia are consistent with the pattern produced by cooling of the lithosphere rather than flexure caused by a subduction zone. The subsidence patterns are similar for wells >1000 km apart, in the direction across strike from the trend of the underlying orogenic belts. Additionally, the individual curves do not have the convex-up shape characteristic of tectonic subsidence curves for foreland basins (Allen and Allen, 2005).The backstripped subsidence curves fit the subsidence from the forward model for most of the timespan.

The wells in Fig. 7 are ordered from west to east and the best fitting models show a trend of a thicker final lithosphere in the west (154 km – Walkandi 1; Fig. 7A) than the east (122 km – Arlington 1; Fig. 7E). This agrees with the trend seen in surface wave tomography (Fishwick et al., 2008). Their results suggest a lithosphere of 150-200 km in the west which is in good agreement with the results of this study, however they only have a ~100 km thick lithosphere in the east which is thinner than the 120 km used in the best fitting model. The crustal thicknesses used in the model also fit reasonably well with those measured. The Moho depth beneath the Eromanga Basin is between 36-40 km (38 km – Walkandi forward model) and 34-36 km beneath the Surat Basin (34 km – Red Cap 1, 32 km – Arlington 1 forward models) (Collins et al., 2003). While the modelled subsidence does not explain the increased subsidence rates seen in the Late Cretaceous it does provide a good fit up to this point.

5. Discussion

Holt et al., (2010) showed that cooling and thickening of the lithosphere provided a good fit to the subsidence of two North African basins in a specific case study. This paper provides further evidence supporting this subsidence mechanism, and shows it is likely to be an inherent property of accretionary crust on a global scale.

Several other mechanisms have been suggested to explain the formation of the basins in this study. Rifting in some form has been suggested for the basins in North Africa (Lüning et al., 1999), South America (Oliveira and Mohriak, 2003), Turan (Thomas et al., 1999) and Australia (Korsch et al., 1988). A typical scenario is that the basins represent thermal subsidence following a conventional phase of extension. In some of the study areas there are indeed rifts visible on seismic data in some of the basins, but, they are only detected locally (e.g. Nikishin et al., 2001). It is possible that other rifts have not yet been discovered. However, many of the basins in this study are producing hydrocarbons or are actively being explored and extensive seismic data exist, so it is unlikely this is the case.

The mechanism of 'slow rifting' involves stretching at low strain rates over a long period of time (Allen and Armitage, 2011; Armitage and Allen, 2010). This produces a subsidence pattern which is initially linear during the slow stretching phase, with a kink when stretching ceases, followed by a decaying curve due to the thermal relaxation phase. When the first points on a subsidence curve are poorly dated it is difficult to distinguish between this 'slow rift' mechanism and the model proposed in this paper. This is the case in South Africa and for the Turan platform. However, in Australia the dating is good enough to show that the subsidence profiles are curved throughout for wells Arlington 1 and Walkandi 1, without an initial linear, slow rift phase, but consistent with the exponential decay of a thermal subsidence curve. The composite well from the Ghadames Basin backstripped in Holt et al, (2010) also has good age resolution for the first data points and is curved throughout. The

caveat that applies to conventional rifting also applies to this slow rift mechanism: there is a lack of imaged rifts in the basins. Armitage and Allen (2010) argued that slow rifting may result in deformation being spread over numerous small faults, which is why they are not imaged. This does not agree with the results from analogue models of rifting which show that lower strain rates lead to increased localisation of strain on fewer large faults (Bellahsen et al., 2003). The same has been observed for active rifts such as the East African rift (Mazzarini et al., 2004).

Slow rifting also requires the basin to be under tension for long periods of time whereas many of the basins show periods of compression in their history. This does not present a problem for cooling and thickening of the lithosphere because it acts in the background and certain times in the basin's history may be influenced by compressional processes, but when these cease the subsidence will continue.

Dynamic topography has also been suggested as a mechanism for forming intracontinental basins of the type analysed here (e.g. Gurnis, 1992; Heine et al., 2008). This model invokes subsidence caused by mantle flow patterns, for example in eastern Australia (Gallaher et al., 1994; Gurnis et al., 1998; Matthews et al,. 2011), but there are problems with its application to the basins in this study. First, there is no obvious reason why mantle downwellings would produce basin subsidence patterns that so closely mimic the thermal subsidence histories found in global examples, i.e. a negative exponential decay. Second, many applications of dynamic topography invoke subduction initiation for the generation of subsidence (Gurnis, 1992), whereas the geological record indicates that basin development begins after subduction has ended under an area.

Avigad and Gvirtzman (2009) produced a model for the subsidence of the Arabian-Nubian Shield that involved thermal subsidence, following loss of the entire mantle lithosphere. For this model to have generic implications, all such intracontinental basins would likewise need to

follow catastrophic delamination. We know of no direct evidence that this has occurred; instead small-scale convection beneath young orogens may be a common process (Kaislaniemi et al., 2014), but not producing regional or even local subsidence.

6. Conclusions

This study worked from the hypothesis that accretionary crust begins with thin underlying mantle lithosphere, which is a property of its origin by processes that favour near-normal crustal thickness, but not the generation of a complementary mantle keel. Subsequent cooling and thickening of the mantle lithosphere causes subsidence as an isostatic response. This basin forming mechanism was shown to be a viable formation mechanism for the Palaeozoic basins of North Africa in Holt et al (2010), with good agreement between forward modelling and backstripped subsidence curves. The present paper shows that the modelled subsidence from this mechanism fits the observed subsidence patterns of basins formed upon accretionary crust from around the world, suggesting that the mechanism is generically applicable to such crust.

Acknowledgements

We thank Statoil for the funding of PJH's original PhD project, and H.M. Bjørnseth for his support. We thank Fred Beekman and an anonymous referee for their helpful and constructive reviews.

References

Abdelsalam, M.G., Liégeois, J.P., Stern, R.J., 2002. The Saharan metacraton. In: Fritz, H., Loizenbauer, J. (Eds.), 18th colloquium of African Geology Journal of African Earth Sciences. Graz Austria. Elsevier, pp. 119–136.

Al-Juboury, A. I., Al-Hadidy, A. H., 2009. Petrololgy and depositional evolution of the Paleozoic rock of Iraq. Marine and Petroleum Geology 26, 208-231.

Al-Mishwat, A. T., Nasir, S. J., 2004. Composition of the lower crust of the Arabian Plate: a xenolith perspective. Lithos 72, 45-72.

Allen, P.A., Allen, J., 2005. Basin Analysis: Principles and Applications. Oxford, Blackwell Publishing.

Allen, P., Armitage, J. J., 2011. Cratonic Basins, In: Busby, C. J., and Pérez, A. A., (Eds.), Tectonics of sedimentary basins: Recent Advances. Cambridge, Wiley-Blackwell Science, pp. 602-620.

Almeida, F. F. M. d., Brito Neves, B. B. d., Carneiro, C. D. R., 2000. The origin and evolution of the South American Platform. Earth Science Reviews 50, 77-111.

Arcay, D., Doin, M.-P., Tric, E., Bousquet, R., de Capitani, C., 2006. Overriding plate thinning in subduction zones. Localised convection induced by slab dehydration. Geochemistry Geophysics Geosystems 7, Q02007, doi: 10.1029/2005GC001061.

Armitage, J. J., Allen, P. A., 2010. Cratonic basins and the long-term subsidence history of continental interiors. Journal of the Geological Society of London 167, 61-70.

Ashwal, L. D., Burke, K., 1989. African lithospheric structure, volcanism and topography. Earth and Planetary Science Letters 96, 8-14.

Avigad, D., Gvirtzman, Z., 2009. Late Neoproterozoic rise and fall of the northern Arabian-Nubian shield: The role of lithospheric mantle delamination and subsequent thermal subsidence. Tectonophysics 477, 217-228.

Begg, G.C., Griffin, W.L., Natapov, L.M., O'Reilly, S.Y., Grand, S.P., O'Neill, C.J., Hronsky, J.M.A., Djomani, Y.P., Swain, C.J., Deen, T., Bowden, P., 2009. The lithospheric architecture of Africa: Seismic tomography, mantle petrology, and tectonic evolution. Geosphere 5, 23-50.

Bellahsen, N., Daniel, J.-M., Bollinger, L., Burov, E., 2003. Influence of viscous layers on the growth of normal faults; insights from experimental and numerical models. Journal of Structural Geology 25, 1471-1485.

Best, J. A., Barazangi, M., Al-Saad, D., Sawaf, T., Gebran, A., 1993. Continental margin evolution of the Northern Arabian platform in Syria. AAPG Bulletin 77, 173-193.

Brito Neves, B. B. d., 2002. Main stages of the development of the sedimentary basins of South America and their relationship with the tectonics of supercontinents. Gondwana Research 4, 175-196.

Bumby, A. J., Guiraud, R., 2005. The geodynamic setting of the Phanerozoic basins of North Africa. Journal of African Earth Sciences 43, 1-12.

Burke, K., MacGregor, D.S., Cameron, N.R., 2003. Africa's petroleum systems: four tectonic 'Aces' in the past 600 million years. In: Arthur, T., MacGregor, D.S., Cmeron, N.R. (Eds.) Petroleum Geology of Africa: New Themes and Developing Technologies, vol. 207, Special Publications. Geological Society, London, pp. 21-60.

Caby, R., Monié, P., 2003. Neoproterozoic subductions and differential exhumation of western Hoggar (southwest Algeria): new structural, petrological and geochronological evidence. Journal of African Earth Sciences 37, 269-293.

Canil, D., 2008. Canada's craton: A bottoms-up view. GSA Today 18, 4-10.

Catuneanu, O., 2004. Retroarc foreland systems - evolution through time. Journal of African Earth Sciences 38, 225-242.

Cawood, P.A., Kroner, A., Collins, W.J., Kusky, T.M., Mooney, W.D., Windley, B.F., 2009. Accretionary orogens through Earth history, In: Cawood, P.A., Kroner, A. (Eds.), Earth Accretionary Systems in Space and Time. Geological Society Publishing House, Bath, pp. 1-36.

Cloetingh, S. A. P. L., Lankreijer, A., de Wit, M. J., Martinez, I., 1992. Subsidence history analyses and forward modelling of the Cape and Karoo Supergroups, In: de Wit, M. J., Ransome, I. D., (Eds.), Inversion tectonics of the Cape Fold Belt, Karoo and Cretaceous basins of Southern Africa. Rotterdam, A. A. Balkema, pp. 239-248.

Collins, C. D. N., Drummond, B. J., Nicoll, M. G., 2003. Crustal thickness patterns in the Australian continent, In: Hills, R. R., Müller, R. D., (Eds.), Evolution and Dynamics of the Australian Plate, Volume 372. Boulder, Colarado, Geological Society of America Special Paper, pp. 121-128.

Collins, W.J., Belousova, E.A., Kemp, A.I.S., Murphy, J.B., 2011. Two contrasting Phanerozoic orogenic systems revealed by hafnium isotope data. Nature Geoscience 4, 333-337.

Debayle, E., Kennett, B.L.N., 2003. Surface-wave studies of the Australian region. In: Hillis, R.R., Müller, R.D., (Eds.), Evolution and Dynamics of the Australian Plate, vol. 372, Boulder, Geological Society of America Special Publications, p.25-40.

Eberle, M. A., Grasset, O., Sotin, C., 2002. A numerical study of the interaction between the mantle wedge, subducting slab, and overriding plate. Physics of the Earth and Planetary Interiors 134, 191-202.

Eyles, C. H., Eyles, N., Franca, A. B., 1993. Glaciation and tectonics in an active intracratonic basin: the Late Palaeozoic Itararé Group, Paraná Basin, Brazil. Sedimentology 40, 1-25.

Feng, M., van der Lee, S., Assumpção, M., 2007. Upper mantle structure of South America from joint inversion waveforms and fundamental mode group velocities of Rayleigh waves. Journal of Geophysical Research 112, 1-16.

Fischer, K.M., 2002. Waning buoyancy in the crustal roots of old mountains. Nature 417, 933-936.

Fishwick, S., Heintz, M., Kennett, B. L. N., Reading, A. M., Yoshizawa, K., 2008. Steps in lithospheric thickness within eastern Australia, evidence from surface wave tomography. Tectonics 27, 1-17.

Frimmel, H. E., Frank, W., 1998. Neoproterozoic tectno-thermal evolution of the Gariep Belt and its basement, Namibia and South Africa. Precambrian Research 90, 1-28.

Gallagher, K., Demitru, T. A., Gleadow, A. J. W., 1994. Constraints on the vertical motion of eastern Australia during the Mesozoic. Basin Research 6, 77-94.

Garfunkel, Z., 2002. Early Paleozoic sediments of NE Africa and Arabia: Products of continental-scale erosion, sediment transport and deposition. Israeli Journal of Earth Sciences 51, 135-156.

Gee, D.G., Stephenson, R.A., 2006. The European lithosphere: an introduction. In: Gee, D.G., Stephenson, R.A., (Eds.), European Lithosphere Dynamics, Vol. 32, London, Geological Society Memoirs, p. 1-9.

Glen, R. A., 2005. The Tasmanides of Eastern Australia, In: Vaughan, A. P. M., Leat, P. T., Pankhurst, R. J., (Eds.), Terrane Process at the Margins of Gondwana, Volume 246, Geological Society, London, Special Publications, pp. 23-96.

Glen, R.A., 2013. Refining accretionary orogen models for the Tasmanides of eastern Australia. Australian Journal of Earth Sciences 60, 315-370.

Guiraud, R., Bosworth, W., 1999. Phanerozoic geodynamic evolution of northeastern Africa and the northwestern Arabian platform. Tectonophysics 315, 73-108.

Gurnis, M., 1992. Rapid continental subsidence following the initiation and evolution of subduction. Science 255, 1556-1558.

Gurnis, M., Muller, R.D., Moresi, L., 1998. Cretaceous vertical motion of Australia and the Australian-Antarctic discordance. Science 279, 1499-1504.

Hansen, S. E., Rodgers, A. J., Schwartz, S. Y., Al-Amri, A. M. S., 2007. Imaging ruptured lithosphere beneath the Red Sea and Arabian Peninsula. Earth and Planetary Science Letters 259, 256-265.

Haq, B.U., Schutter, S.R., 2008. A chronology of Paleozoic sea-level changes. Science 322, 64-68.

Heine, C., Müller, R. D., Steinberger, B., Torsvik, T. H., 2008. Subsidence in intracontinental basins due to dynamic topography. Physics of the Earth And Planetary Interiors 171, 252-264.

Holt, P., Allen, M. B., van Hunen, J., Bjørnseth, H. M., 2010. Lithospheric cooling as a basin forming mechanism within accretionary crust. Tectonophysics 495, 184-194.

Huang, J., and S. Zhong (2005), Sublithospheric small-scale convection and its implications for the residual topography at old ocean basins and the plate model, J. Geophys. Res., 110, B05404, doi:10.1029/2004JB003153

Hyndman, R.D., Currie, C.A., Mazzotti, S.P., 2005. Subduction zone backarcs, mobile belts and orogenic heat. GSA Today 15, 4-10.

Jahn, B.M., Wu, F.Y., Chen, B., 2000. Massive granitoid generation in Central Asia: Nd isotope evidence and implication for continental growth in the Phanerozoic. Episodes 23, 82-92.

Jimenez-Munt, I., Fernandez, M., Saura, E., Verges, J., Garcia-Castellanos, D., 2012. 3-D lithospheric structure and regional/residual Bouguer anomalies in the Arabia-Eurasia collision (Iran). Geophysical Journal International 190, 1311-1324.

Kaislaniemi, L., van Hunen, J., Allen, M.B., Neill, I., 2014. Small-scale convection as the mechanism for generating collision zone magmatism. Geology 42, 291-294.

Konert, G., Afifi, A.M., Al-Hajri, S.A., Droste, H.J., 2001. Paleozoic stratigraphy and hydrocarbon habitat of the Arabian plate. GeoArabia 6, 407-442.

Korsch, R. J., Harrington, H. J., Wake-Dyster, K. D., O'Brien, P. E., Finlayson, D. M., 1988. Sedimentary basins peripheral to the New England Orogen: their contribution to understanding New England tectonics, In: Kleeman, D., (Ed.), New England Orogen, Tectonics and Metallogenesis. Armidale, Australia, University of New England, pp. 134-140.

Kusky, T.M., Windley, B.F., Safonova, I., Wakita, K., Wakabayashi, J., Polat, A., Santosh, M., 2013. Recognition of ocean plate stratigraphy in accretionary orogens through Earth history: A record of 3.8 billion years of sea floor spreading, subduction, and accretion. Gondwana Research 24, 501-547.

Liégeois, J. P., Black, R., Navez, J., Latouche, L., 1994. Early and Later Pan-African orogenies in the Aïr assembly of terranes (Tuareg shield, Niger). Precambrian Research 67, 59-88.

Lüning, S., Craig, J., Fitches, B., Mayouf, J., Busrewil, A., El Dieb, M., Gammudi, A., Loydell, D., McIlroy, D., 1999, Re-evaluation of the petroleum potential of the

Kufra Basin (SE Libya, NE Chad): does the source rock barrier fall? Marine and Petroleum Geology 16, 693-718.

Matthews, K.J., Hale, A.J., Gurnis, M., Muller, R.D., DiCaprio, L., 2011. Dynamic subsidence of Eastern Australia during the Cretaceous. Gondwana Research 19, 372-383.

Mazzarini, F., Corti, G., Mazzarini, F., Corti, G., Manetti, P., Innocenti, F., 2004. Strain rate and bimodal volcanism in the continental rift: Debre Zeyt volcanic field, northern MER, Ethiopia. Journal of African Earth Sciences 39, 415-420.

McGillivray, J. G., Husseini, M. I., 1992. The Palaeozoic petroleum geology of Central Arabia. AAPG Bulletin 76, 1473-1490.

McKenzie, D., 1978. Some remarks on the development of sedimentary basins. Earth and Planetary Science Letters 40, 25-32.

McKenzie, D., Jackson, J., Priestley, K., 2005. Thermal structure of oceanic and continental lithosphere. Earth and Planetary Science Letters 233, 337-349.

Milani, E. J., De Wit, M. J., 2008. Correlations between the classic Paraná and Cape - Karoo sequences of South America and southern Africa and their basin infills flanking the Gondwanides: du Toit revisited, In: Pankhurst, R. J., Trouw, R. A. J., Brito Neves, B. B., De Wit, M. J., (Eds.), Pre-Cenozoic correlations across the South Atlantic region, vol. 294. Special Publications. Geological Society, London, 319-342.

Natal'in, B. A., Şengör, A. M. C., 2005. Late Palaeozoic to Triassic evolution of the Turan and Scythian platforms; the pre-history of the palaeo-Tethyan closure. Tectonophysics 404, 175-202.

Neves, B.B.D., Fuck, R.A., 2013. Neoproterozoic evolution of the basement of the South-American platform. Journal of South American Earth Sciences 47, 72-89.

Nikishin, A. M., Ziegler, P. A., Panov, D. I., Nazarevich, B. P., Brunet, M.-F., Stephenson, R. A., Bolotov, S. N., Korotaev, M. V., Tikhomirov, P. L., 2001. Mesozoic and Cainozoic evolution of the Scythian Platform - Black Sea - Caucasus domain, In: Ziegler, P. A., Cavazza, W., Robertson, A. H. F., Crasqui-Soleau, S., (Eds.), Peri-Tethyan rift/wrench basins and passive margins, Volume 6. Paris, Mémoires du Muséum national d'Histoire Naturelle, pp. 295-346.

Oliveira, D. C. d., Mohriak, W. U., 2003. Jaibaras trough: an important element in the early tectonic evolution of the Parnaíba interior sag basin, Northern Brazil. Marine and Petroleum Geology 20, 351-383.

Park, Y., Nyblade, A. A., Rodgers, A. J., Al-Amri, A., 2008. S wave velocity structure of the Arabian Shield upper mantle from Rayleigh wave tomography. Geochemistry Geophysics Geosystems, 9, Article Number Q07020.

Parsons, B., Sclater, J.G., 1977. An analysis of the variation of of the ocean floor bathymetry and heat flow with age. Journal of Geophysical Research, 108, 803-827.

Pasyanos, M. E., 2010. Lithospheric thickness modeled from long-period surface wave dispersion. Tectonophysics 481, 38-50.

Pasyanos, M. E., Nyblade, A. A., 2007. A top to bottom lithospheric study of Africa and Arabia. Tectonophysics 444, 27-44.

Priestley, K., McKenzie, D., 2006. The thermal structure of the lithosphere from shear wave velocities. Earth and Planetary Science Letters 244, 285-301.

Sclater, J.G., Christie, P.A.F., 1980. Continental stretching; an explanation of the post-Mid-Cretaceous subsidence of the central North Sea basin. Journal of Geophysical Research 85, 3711-3739.

Şengör, A.M.C., Natal'in, B.A., 1996. Paleotectonics of Asia: fragments of a synthesis., In: Yin, A., Harrison, M. (Eds.), The Tectonic Evolution of Asia. Cambridge University Press, Cambridge, pp. 486-640.

Stern, R. J., 1994. Arc assembly and continental collision in the Neoproterozoic East African orogen: Implications for the consolidation of Gondwanaland. Annual Review of Earth and Planetary Science 22, 319-351.

Tankard, A., Welsink, H., Aukes, P., Newton, R., Stettler, E., 2009. Tectonic evolution of the Cape and Karoo basins of South Africa. Marine and Petroleum Geology 26, 1379-1412.

Thomas, J. C., Cobbold, R., Shein S., Le Douaran, S., 1999. Sedimentary record of late Paleozoic to Recent tectonism in central Asia - analysis of subsurface data from the Turan and south Kazak domains. Tectonophysics 313, 243-263.

Turcotte, D. L., Schubert, G., 2002. Geodynamics, Cambridge, Cambridge University Press.

Turner, B. R., Armstrong, H. A., Holt, P., 2011. Visions of ice sheets in the early Ordovician greenhouse world: Evidence from the Peninsula Formation, Cape Peninsula, South Africa. Sedimentary Geology 236, 226-238.

Van Hinsbergen, D.J.J., Buiter, S.J.H., Torsvik, T.H., Gaina, C., Webb, S.J., 2011. The formation and evolution of Africa from the Archaean to Present: introduction. In: Van Hinsbergen, D.J.J., Buiter, S.J.H., Torsvik, T.H., Gaina, C., Webb, S.J., (Eds.), Vol. 357: London, Geological Society Special Publications, p. 1-8.

van Hunen, J., Zhong, S., Shapiro, N.M., Ritzwoller, M.H., 2005. New evidence for dislocation creep from 3-D geodynamic modeling of the Pacific upper mantle structure. Earth and Planetary Science Letters 238, 146-155.

van Keken, P. E., 2003. The structure and dynamics of the mantle wedge. Earth and Planetary Science Letters Frontiers 215, 323-338.

Veevers, J.J., 2006. Updated gondwana (Permian-Cretaceous) earth history of Australia. Gondwana Research 9, 231-260.

Watts, A. B., Ryan, W. B. F., 1976. Flexure of the lithosphere and continental margin basins. Tectonophysics 36, 25-44.

Williams, H., Hoffman, P.F., Lewry, J.F., Monger, J.W.H., Rivers, T., 1991. Anatomy of North America: thematic geologic portrayals of the continent. Tectonophysics 187, 117-134.

Xiao, W., Windley, B.F., Badarch, G., Sun, S., Li, J., Qin, K., Wang, Z., 2004. Palaeozoic accretionary and convergent tectonics of the southern Altaids: implications for the growth of Central Asia. Journal of the Geological Society 161, 339-342.

Zalán, P. V., Wolff, S., Astolfi, M. A. M., Vieira, I. S., Concelção, J. C. J., Appi T., Neto, E. V. S., Cerqueira, J. R., Marques, A., 1990. The Paraná Basin, Brazil, In: Leighton, M. W., Kolata, D. R., Oltz, D. F., Eidel, J. J., (Eds.), Interior Cratonic Basins. AAPG memoir 51. Tulsa Oklahoma, pp. 681-708.

Zhao, D., Hasegawa, A., Kanamori, H., 1994. Deep structure of Japan subduction zone as derived from local, regional, and teleseismic events. Journal of Geophysical Research 99, 22313-22329.

Zor, E., Sandvol, E., Gürbüz, C., Türkelli, N., Seber, D., Barazangi, M., 2003. The Crustal structure of the East Anatolian plateau (Turkey) from receiver functions. Geophysical Research Letters 30, 8044-8048.

Figure captions

Fig. 1. Age of assembly of continental crust. This is not necessarily the age of the units within each area, but the age at which that region of crust was assembled as a unit. This is a compilation of data from numerous publications covering South America (Almeida et al., 2000; Milani and De Wit, 2008), North America (Canil, 2008; Williams et al., 1991), Europe (Gee and Stephenson, 2006), Africa and Arabia (Begg et al., 2009; Van Hinsbergen et al., 2011), Asia (Şengör and Natal'in, 1996) and Australia (Debayle and Kennett, 2003).

Fig. 2. Locations of basins, wells and pseudo-wells in this study; (a) Location map of the Palaeozoic intracratonic basins in South America. Wells from the Paraná Basin from Milani and De Wit (2008) and Zalán et al (1990); (b) The extent of the Cape-Karoo Basin of South Africa (Tankard et al., 2009). The location of the outcrop sections used to make up the subsidence curve for the Cape Fold Belt is shown by the circle. The composite sections used by Cloetingh et al (1992) are used for pseudo-wells Cape 1 and Cape-Karoo 2, representative of west of 20^{o} E (Western Cape) and east of 24^{o} E (Southeastern Cape); (c) The extent of sediments beneath the Hercynian unconformity (roughly Late Carboniferous in age) across Arabia. The location of the Khanaser #1 well in Syria and the outcrop study used for the backstripping are both located upon the map; (d) A map of the sedimentary cover over the Turan and Scythian platforms take from (Natal'in and Şengör, 2005; Thomas et al., 1999). In the absence of usable well data a cross-section (Thomas et al., 1999) has been used as input for the backstripping. The location of the cross-section is shown on the map. The four 'pseudo wells' from the cross-section are marked; (e) The Mesozoic-Cenozoic cover of Eastern Australia. The extent of the sedimentation is taken from Gallagher et al. (1994). The location of the depocentres mentioned in the text and the wells used in the backstripping are shown on the map. The abbreviations for each of the wells are as follows. W = Walkandi 1, C = Cook North 1, L = Lowood 1, R = Red Cap 1 and A = Arlington 1.

Fig. 3. The backstripped subsidence curves for the Paraná Basin and the PreCordillera compared with the best fitting forward models. The sources of the three curves from the Paraná Basin are explained in the text, and wells for the Paraná Basin are located on Fig. 2a. Well A is from the PreCordillera, B and C are from the main Paraná Basin, using data in Milani and DeWit (2008) and versions of the stratigraphy from both Zalán et al (1990) and Eyles et al (1993). The best fitting model for the Paraná Basin has a 36 km crust and a final lithosphere thickness of 130 km. The PreCordillera is best fitted by a model with a 30 km thick crust, but the same final lithosphere thickness.

Fig. 4. Backstripped subsidence curves from the outcrop data in the Cape Fold Belt (A) and from two pseudo wells in the wider Cape-Karoo Basin (B and C). See Fig. 2b for location information. The best fit forward models to each of these subsidence curves are shown alongside the backstripping. All the best fit models have a final lithospheric thickness of 122 km. The Cape Fold Belt is fitted by a 23 km thick crust and the wider Cape-Karoo Basin by a 27 km thick crust.

Fig. 5. The Palaeozoic sediments of Arabia contain a number of eroded sections which shows in the backstripped subsidence curves as flat areas with no subsidence. The best fitting subsidence curves from the forward model are shown alongside the backstripping. The Khanaser #1 well (A) is fitted best by a 30 km thick crust and 122 km thick final lithosphere. The outcrop data are fitted best by a 33 km thick crust and a 139 km lithosphere (B). Locations of the well and outcrop data are shown on Fig. 2c.

Fig. 6. The results of the backstripping from the four pseudo-wells in the Turan platform (located on Fig. 2d). The best fitting models for each well all have a final lithospheric thickness of 155 km. The best fitting crustal thickness for the Khiva Depression (A) is 28 km, 30 km is used for both Amu Dar'ya 1 and 2 (B and C) and a 31 km thick crust is used for Chardhzu (D).

Fig. 7. The backstripped subsidence curves from the platformal succession of Eastern Australia compared to the curves produced by the best fitting forward model. The locations of the wells are shown on Fig. 2e. The best fitting model varies from Walkandi 1 well in the west which is fitted best by a model with a 154 km thick lithosphere and a 38 km thick crust (A). The best fitting crust gets thinner as does the lithosphere to the east, through the Cook North 1 (B), Lowood 1 (C) and Red Cap 1 (D) wells, with the Arlington 1 well (E) being fitted best by a 32 km thick crust and a 122 km thick final lithosphere.

Figure

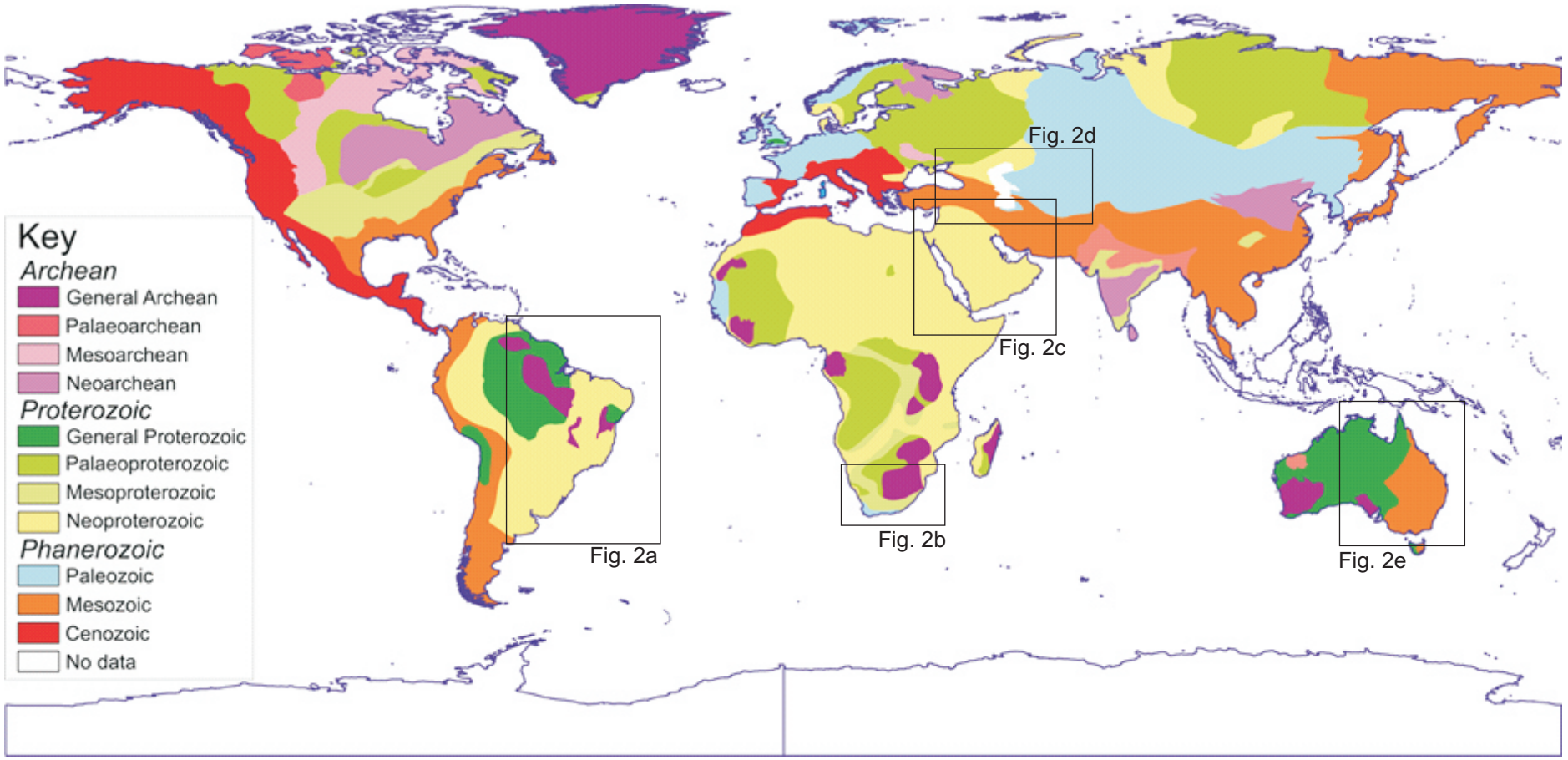

Figure 1

Figure

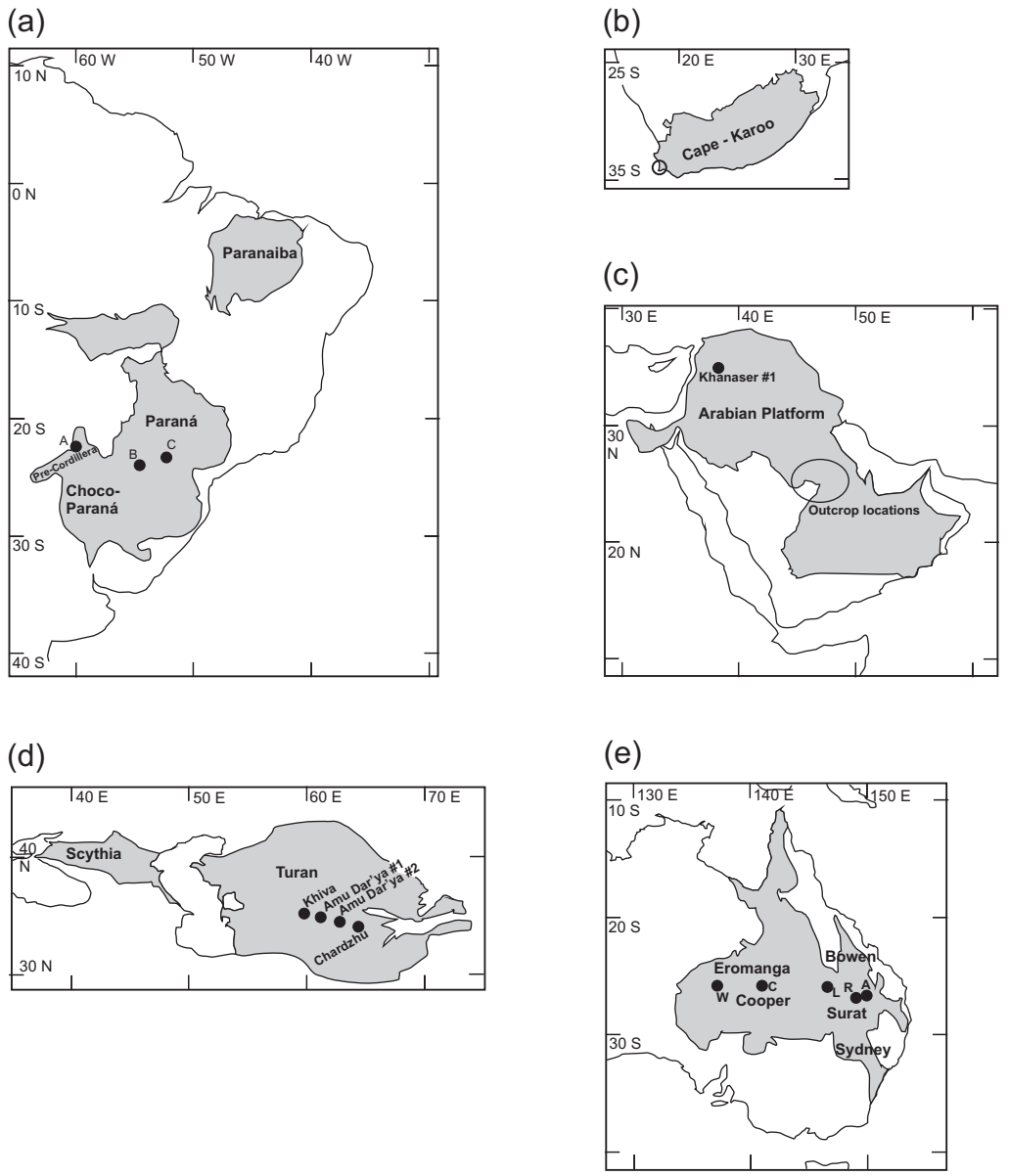

Figure 2

Figure

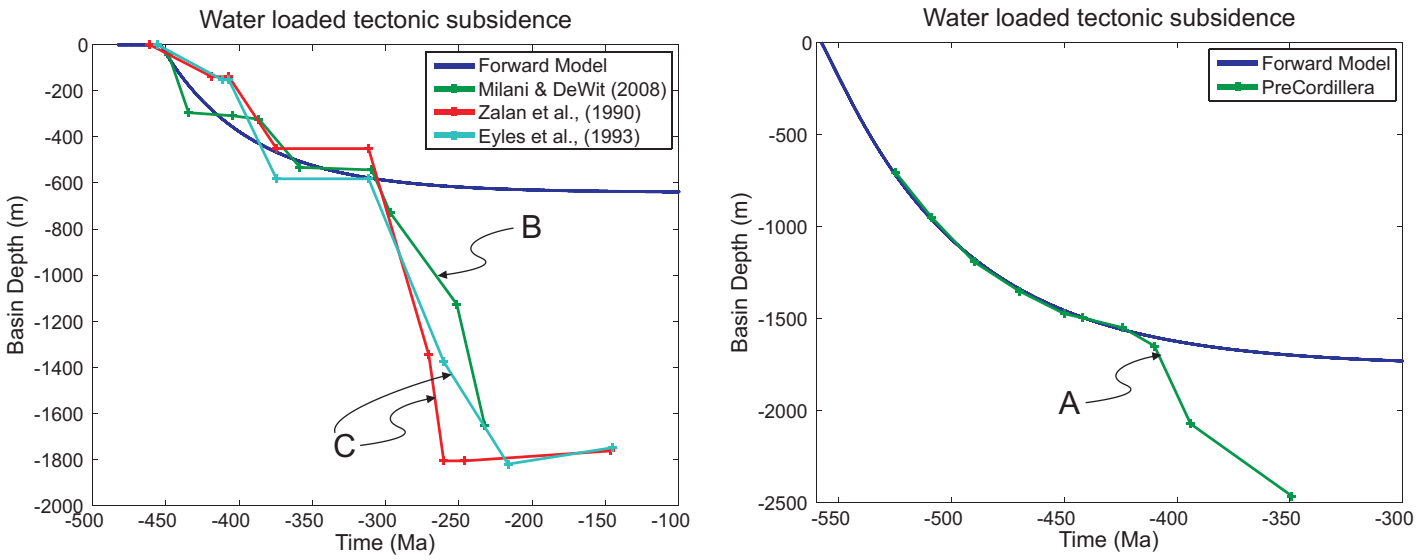

Figure 3

Figure

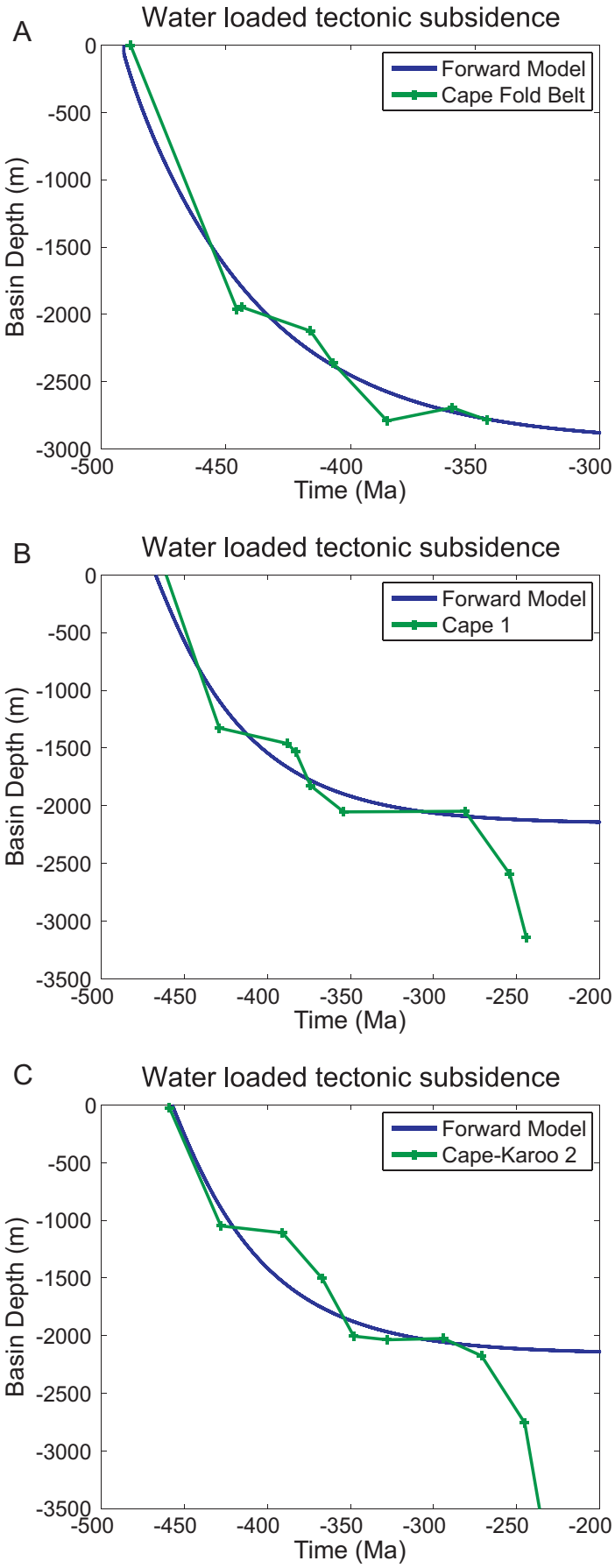

Figure 4

Figure

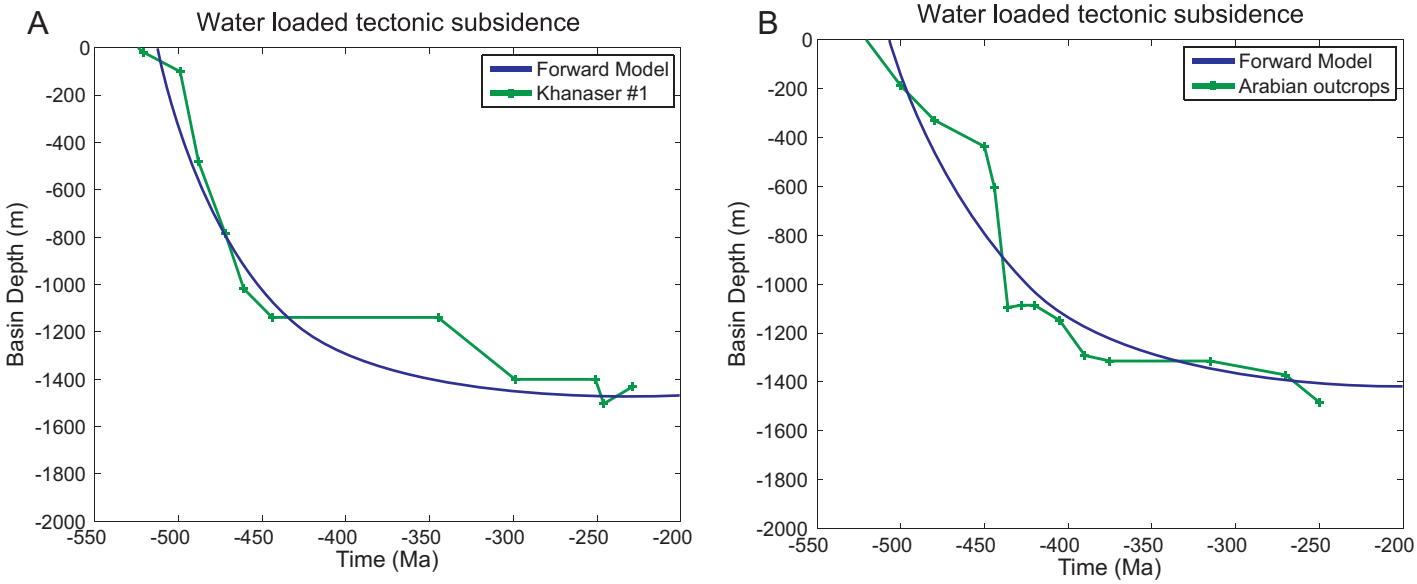

Figure 5

Figure

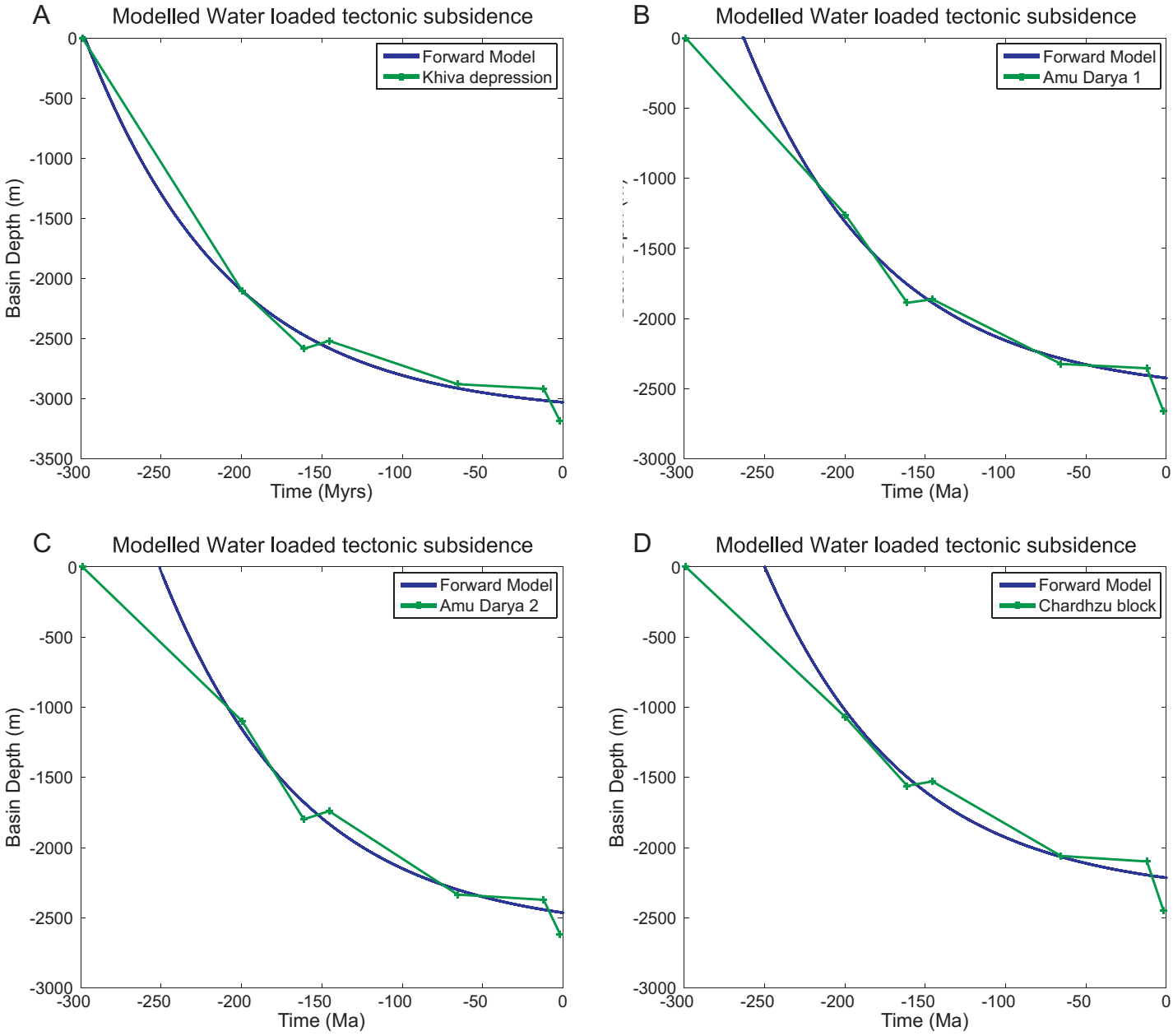

Figure 6

Figure

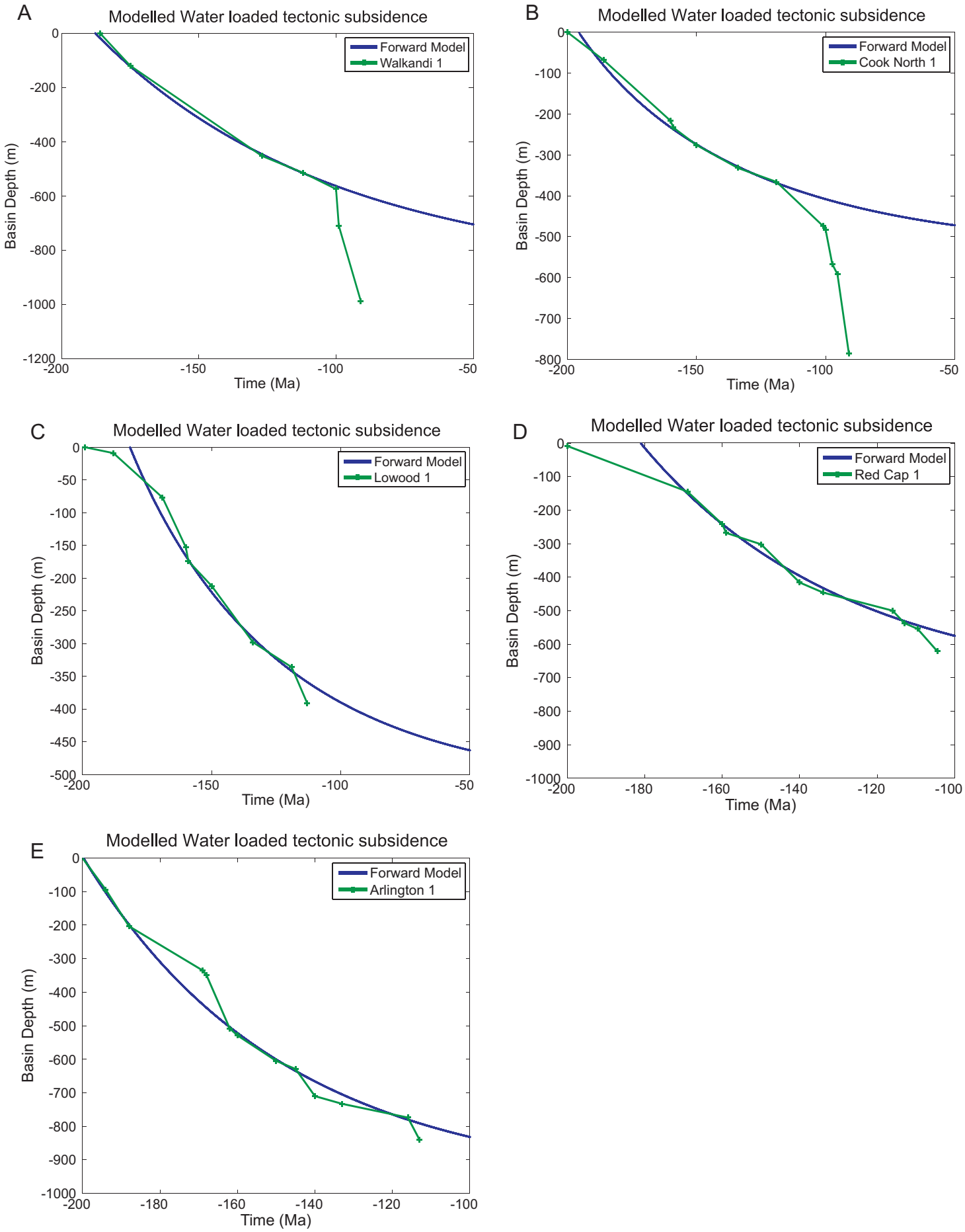

Figure 7